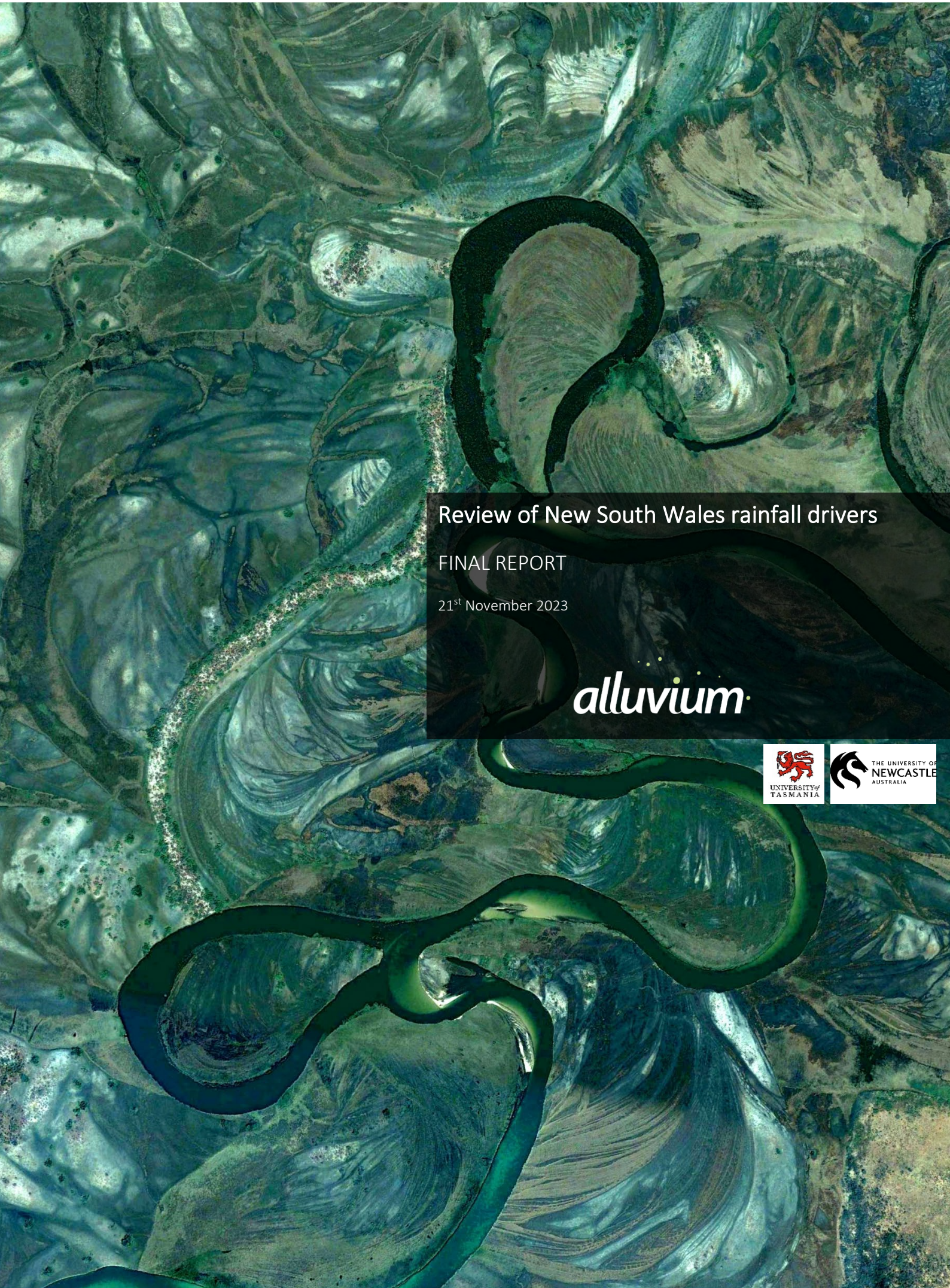

Review of New South Wales rainfall drivers

FINAL REPORT

21st November 2023

alluvium

UNIVERSITY of TASMANIA

THE UNIVERSITY OF NEWCASTLE AUSTRALIA

Alluvium recognises and acknowledges the unique relationship and deep connection to Country shared by Aboriginal and Torres Strait Islander people, as First Peoples and Traditional Owners of Australia. We pay our respects to their Cultures, Country and Elders past and present.

Artwork by Melissa Barton. This piece was commissioned by Alluvium and tells our story of caring for Country, through different forms of waterbodies, from creeklines to coastlines. The artwork depicts people linked by journey lines, sharing stories, understanding and learning to care for Country and the waterways within.

This report has been prepared by Alluvium Consulting Australia Pty Ltd and the University of Tasmania for **The Department of Planning and Environment (New South Wales Government)** under the contract titled '**Review of NSW rainfall drivers**'.

Authors:	Danielle Udy, Anthony Kiem, Tessa Vance
Review:	Anthony Kiem, Tessa Vance
Approved:	Danielle Udy
Version:	3 – final with alt-text
Date issued:	21st November 2023
Issued to:	Richard Beecham, DPE Department Reference Number: PUB24/332
Citation:	Alluvium, 2023, Review of NSW rainfall drivers, report prepared by Alluvium Consulting Australia, the University of Tasmania and the University of Newcastle for the Department of Planning and Environment, Parramatta, NSW
Cover image:	abstract river image, Shutterstock

alluvium

Contents

Figures

Tables

Abbreviations

CMIP	Coupled Model Intercomparison Projects
ECC	East Coast Cyclones
ECL	East Coast Lows
ENSO	El Niño-Southern Oscillation
GCM	General Circulation Model
IOD	Indian Ocean Dipole (IOD+ = positive IOD, IOD- = negative IOD)
IPO	Interdecadal Pacific Oscillation
MJO	Madden-Julian Oscillation
NARCliM	New South Wales and Australian Capital Territory Regional Climate Model
PDO	Pacific Decadal Oscillation
RCM	Regional climate model
SAM	Southern Annular Mode (SAM+ = positive SAM, SAM- = negative SAM)
SOI	Southern Oscillation Index
SST	Sea Surface Temperature
SSTA	Sea Surface Temperature Anomaly

Glossary

Anthropogenic climate change	Refers to changes of the mean climate (e.g. temperature increases) which is attributed directly or indirectly to human activity that alters the composition of the global atmosphere (e.g. by increasing carbon dioxide concentrations) and which is in addition to natural climate variability observed over comparable periods.
Atmospheric blocking	Large scale (100's to 1000's of kilometres) patterns in atmospheric high pressure that are nearly stationary for up to 10 days and block the usual westerly flowing midlatitude (30°-60° south) storm track. This forces weather systems to detour around the block, either to the north or south.
Atmospheric rivers	Relatively long, narrow regions (several thousand kilometres long and only a few hundred kilometres wide) in the atmosphere – like rivers in the sky – that transport most of the water vapor outside of the tropics.
Autumn	March, April, May
Climate change	Refers to the change in the state of climate that can be identified by changes in the mean and/or the variability of its properties and that persists for an extended period, typically decades or longer. Climate change can be due to natural internal processes or external forcings. External forcings can be natural (e.g. volcanic eruptions can reduce global temperatures for a period of years) or anthropogenic (i.e. human-caused increases in aerosol and greenhouse gas emissions).
Climate variability	Refers to the variations in the mean state or extremes of the climate across spatial and temporal scales beyond that of individual weather events. Variability may be due to internal natural processes within the climate system or associated with natural or anthropogenic external forcing of the change.
Closed cyclonic circulation	Refers to cyclonic / clockwise rotation of atmospheric masses (in the Southern Hemisphere) that forms a closed circulation on weather maps. An example of closed cyclonic circulation would be an east coast low.
Convection	Vertical motion driven by buoyancy forces arising from static instability, usually caused by near-surface cooling or increases in salinity in the case

	of the ocean and near-surface warming in the case of the atmosphere. At the location of convection, the horizontal scale is approximately the same as the vertical scale, as opposed to the large contrast between these scales in the general circulation. The net vertical mass transport is usually much smaller than the upward and downward exchange.
Cool season	May to October conditions (for most of New South Wales)
El Niño-Southern Oscillation (ENSO)	The term El Niño was initially used to describe a warm-water current that periodically flows along the coast of Ecuador and Peru, disrupting the local fishery. It has since become identified with a basin-wide warming of the tropical Pacific Ocean east of the dateline. This oceanic event is associated with a fluctuation of a global-scale tropical and subtropical surface pressure pattern called the Southern Oscillation. This coupled atmosphere-ocean phenomenon, with preferred time scales of ~2-7 years, is collectively known as the El Niño-Southern Oscillation (ENSO). ENSO is often measured by the surface pressure anomaly difference between Darwin and Tahiti and the sea surface temperatures in the central and eastern equatorial Pacific. During an ENSO event, the prevailing trade winds weaken, reducing upwelling and altering ocean currents such that the sea surface temperatures warm, further weakening the trade winds. This event has a great impact on the wind, sea surface temperature, and precipitation patterns in the tropical Pacific. It has climatic effects throughout the Pacific region and in many other parts of the world, through global teleconnections. The cold phase of ENSO is called La Niña.
ERA5 reanalysis	ERA5 combines vast amounts of historical observations into global estimates using advanced modelling and data assimilation systems. It is the 5th generation European Centre for Medium-Range Weather Forecasts (ECMWF) atmospheric reanalysis of the global climate covering the period from January 1940 to present
Fronts	A weather front is a boundary between two air masses. There are three kinds of fronts relevant to Australian climate – cold, warm and occluded. Cold fronts represent conditions where a cold air mass is advancing and pushing underneath warmer air due to cold air being heavier than warm air. Warm fronts represent conditions where a warm air mass is advancing and rising over a cold air mass. An occluded front occurs when a cold front catches up with a warm front.
Hadley Cell	A large-scale atmospheric convection cell in which air rises at the equator and sinks at medium latitudes, typically about 30° north or south of the equator.
Historical scenario	Historical climate runs in CMIP models over the period 1850 to present. These are used to evaluate the performance of models to observational datasets.
Indian Ocean Dipole (IOD)	Large-scale interannual variability of sea surface temperature in the Indian Ocean. This pattern manifests through a zonal gradient of tropical sea surface temperature, which in one extreme phase in boreal autumn shows cooling off Sumatra and warming off Somalia in the west, combined with anomalous easterlies along the equator.
Interdecadal Pacific Oscillation (IPO)	A large-scale, long period oscillation that influences climate variability over the Pacific Basin. The IPO operates at a multi-decadal scale, with phases typically lasting around 10 to 30 years.

Intertropical Convergence Zone	The Intertropical Convergence Zone, or ITCZ, is the region that circles the Earth, near the equator, where the trade winds of the Northern and Southern Hemispheres come together.
Madden-Julian Oscillation (MJO)	The major fluctuation in tropical weather on weekly to monthly timescales. The MJO can be characterised as an eastward moving 'pulse' of cloud and rainfall near the equator that typically recurs every 30 to 60 days.
Modes of climate variability	Coherent patterns persisting over weeks to months and in some cases years. They explain links between the ocean and the atmosphere (referred to as a 'coupled mode') that influence climate variability on seasonal to decadal timescales. While the variability is complex, they are often represented by an index computed from observed changes in the ocean and/or atmosphere through time. including IPO, ENSO, IOD, SAM and MJO.
Observed (or instrumental) record	Historical period for which direct measurements were taken (e.g. with rain gauges).
Orographic rainfall	Refers to rainfall that is produced when moist air is lifted up as it moves over an elevated area (e.g. a mountain range). As the air rises and cools, the water moisture in the air parcel condenses to form clouds and rainfall. An example of orographic rainfall is rainfall that occurs on the eastern side of the Great Dividing Range.
Outgoing longwave radiation	Is the energy emitted from the Earth's surface, oceans and atmosphere in the form of thermal infrared radiation. Areas of increased outgoing longwave radiation indicate enhanced convection, more cloud coverage and rainfall.
Pacific Decadal Oscillation (PDO)	The pattern and time series of the first empirical orthogonal function of sea surface temperature over the North Pacific north of 20°N. PDO broadened to cover the whole Pacific Basin is known as the Inter-decadal Pacific Oscillation (IPO).
Palaeoclimate	Historical climate period for which direct measurements were not taken.
Rossby waves	Large horizontal waves in the atmosphere that form a boundary between cold polar air masses and warm tropical air masses. The location and direction of the wave break explains the location of low and high pressure systems. Rossby waves also interconnect tropical climate variability to mid-latitudes.
Southern Annular Mode (SAM)	Low-frequency mode of atmospheric variability of the southern hemisphere that is defined as a belt of strong westerly winds or low pressure surrounding Antarctica which moves north or south as its mode of variability.
Spring	September, October, November
Summer	December, January, February
Synoptic weather systems	Refers to weather systems with a horizontal length around the order of 1000km, for example high and low pressure systems seen on weather maps. An example is the seasonal high pressure systems that occur in the Great Australian Bight. The word 'synoptic' is derived from the ancient Greek word meaning "seen together".
Thermocline tilt	A thermocline is the transition layer between warmer mixed water at the ocean's surface and cooler deeper water below. This barrier tilts in response to the phase of ENSO (in the Pacific Ocean) and IOD (in the Indian Ocean).

Trade winds	Winds in the tropics generally flow in an east to west direction (easterlies). So called because their consistency facilitated transoceanic sailing and commerce.
Warm season	November to April conditions (for most of NSW)
Winter	June, July, August
Zonal wind	The west to east component of wind direction and strength

1 Introduction

The climate of New South Wales (NSW) is highly variable in space and time, and is subject to a range of natural climate influences as well as the compounding impacts of anthropogenic climate change. It is well known that large-scale modes of tropical and extra-tropical climate variability, such as the Interdecadal Pacific Oscillation (IPO), El Niño-Southern Oscillation (ENSO), Indian Ocean Dipole (IOD) and the Southern Annular Mode (SAM) influence seasonal to multi-decadal variability of rainfall across NSW. Additionally, the presence or absence of rain bearing weather systems including east coast lows and atmospheric rivers impact the flood / drought risk and availability of water across NSW.

Rainfall seasonality varies across NSW (Figure 1), ranging from summer dominated in the northeast subtropical regions (including parts of the Far North Coast, North Coast, Greater Hunter, Border Rivers, Gwydir, Namoi regional water strategy management regions) to winter dominated in the southern temperate regions adjacent to the Victorian border (including Murray and Murrumbidgee management regions). The central temperate regions of the state, including parts of Greater Sydney, South Coast, Macquarie-Castlereagh and Lachlan management regions experience more uniform annual rainfall compared to the northeast and southern regions. The Great Dividing Range, running north to south along the east coast of NSW, also significantly influences rainfall distribution across the state by blocking the flow of moist south-easterly trade winds from the Tasman and Coral Sea. This leads to higher mean annual rainfall along the coastal regions and over the range compared to the inland regions west of the range [1]. The dominant climate drivers of rainfall variability also shift either side of the Great Dividing Range, with rainfall over inland regions having stronger relationships with large scale modes of climate variability such as ENSO compared to the NSW coast [1–3]. Rainfall in the coastal regions have reduced relationships with modes of climate variability due to the confounding influence of local synoptic weather scale events such as East Coast Lows [2]. Rainfall along the eastern seaboard itself is further differentiated by traversing subtropical to temperate zones [2].

The dominant rain bearing weather systems for NSW include both tropical origin systems (i.e. tropical depressions and troughs) and mid-latitude (35-55°S) weather systems (i.e. Tasman Sea high pressure systems, cold fronts, east coast low pressure systems)[4–9].

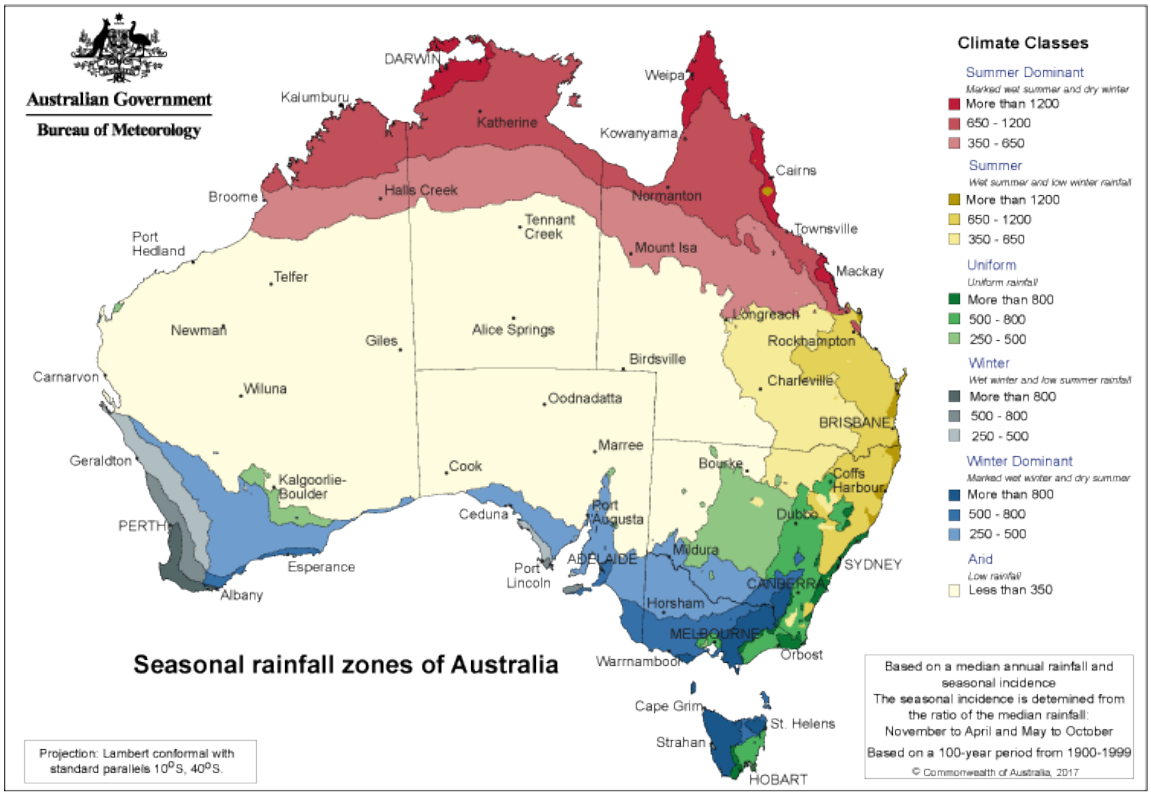

Figure 1: Australian seasonal rainfall zones. The median annual rainfall (based on 100-year period from 1900 to 1999) and seasonal occurrence of rainfall (the ratio of the median rainfall over the period November to April compared to May to October) is used to identify six major zones; summer dominate (wet summer, dry winter), summer (wet summer, low winter rainfall), uniform (no clear seasonality), winter (wet winter, low summer rainfall), winter dominated (wet winter, dry summer) and arid (low annual rainfall). Source: Bureau of Meteorology http://www.bom.gov.au/jsp/ncc/climate_averages/climate-classifications/index.jsp.

This report synthesises the available literature on the influence of the modes of climate variability and weather systems on rainfall across NSW to consolidate the understanding of the climate drivers, their significance for rainfall and any projected changes. This will provide the necessary background information to inform methodology updates in future iterations of regional water strategy planning.

The review includes the following:

- Summary of NSW rainfall variability and trends incorporating both instrumental and palaeoclimate records in Section 2.
- A description of each climate / weather driver and how they influence rainfall variability across NSW. The summary is split between individual influence of climate drivers (Section 3.1), compound influence of climate drivers (Section 3.2) and synoptic-scale weather systems (Section 3.3) important for delivery of rainfall across NSW. The availability of data for these climate drivers and weather systems (past and present) is included in the dataset sections of each driver in Section 3.1 and 3.3.
- The relative importance of the climate and weather drivers over northern, central, and southern regions of coastal and inland NSW are summarised in Section 4.
- Summary of model evaluation studies on the ability of climate models to simulate the climate drivers and associated teleconnections to NSW rainfall in Section 5.
- Projected changes to climate drivers on NSW rainfall in Section 5.

2 Historical variability and trends in NSW rainfall (based on instrumental and palaeoclimate records)

NSW rainfall is highly variable with prolonged periods of below average rainfall interspersed with 2–3-year periods of above average rainfall. Over the observational record (post 1900) there is no significant annual rainfall trend, however rainfall between May and October has decreased over the past two decades. Rainfall reconstructions using palaeoclimate proxies (e.g., tree rings, speleothems, lake sediments and ice cores) indicate that the observational rainfall record underestimates the duration and frequency of wet and dry periods

NSW annual rainfall is highly variable, with area averaged annual rainfall for the state ranging from less than 200mm (in 2019) to greater than 900mm (in 1950). Since 1900, there has been multiple prolonged periods of below average rainfall (less than 556 mm; 1961-1990 average) interspersed with 2–3-year periods of wet conditions (Figure 2). Across the entire state there is no significant annual rainfall trend, however rainfall between April and October has been below average or lowest on record over the past two decades across most of NSW (Figure 3). This is particularly concerning for water availability in the southern NSW catchments which receive most of their rainfall in winter (Figure 1).

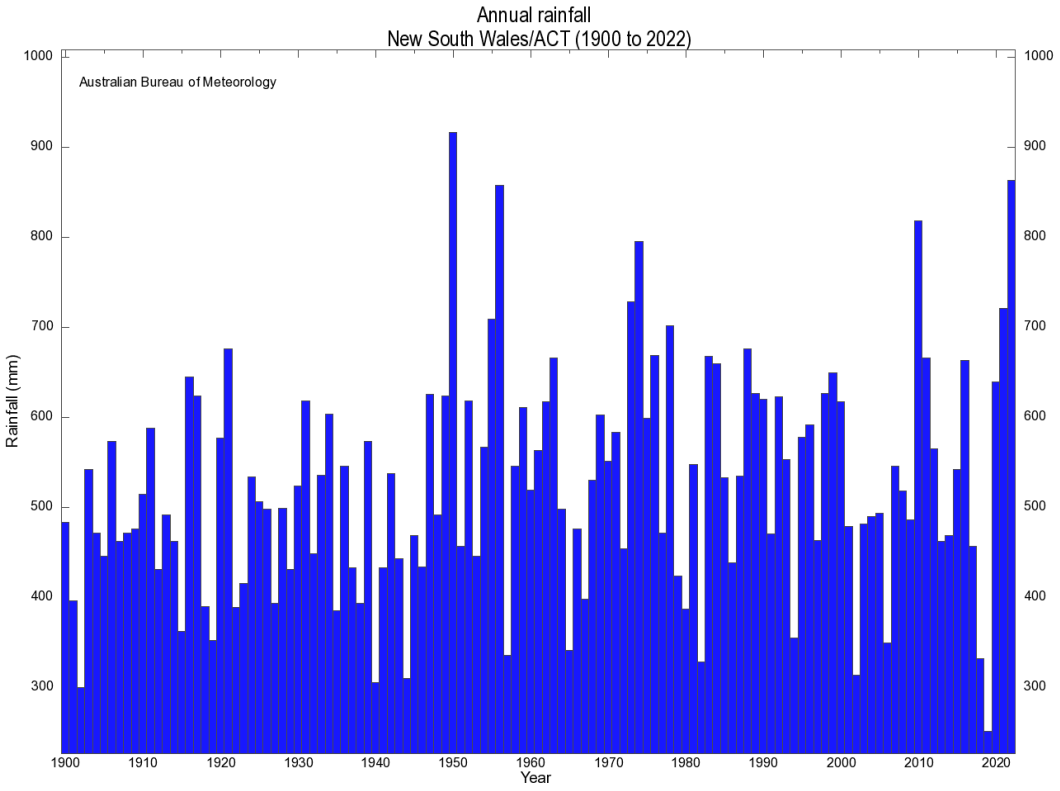

Figure 2: Annual rainfall across New South Wales and Australian Capital Territory between 1900 to 2022. The average rainfall between 1961-1990 is 556.2mm. Source: Bureau of Meteorology; http://www.bom.gov.au/climate/

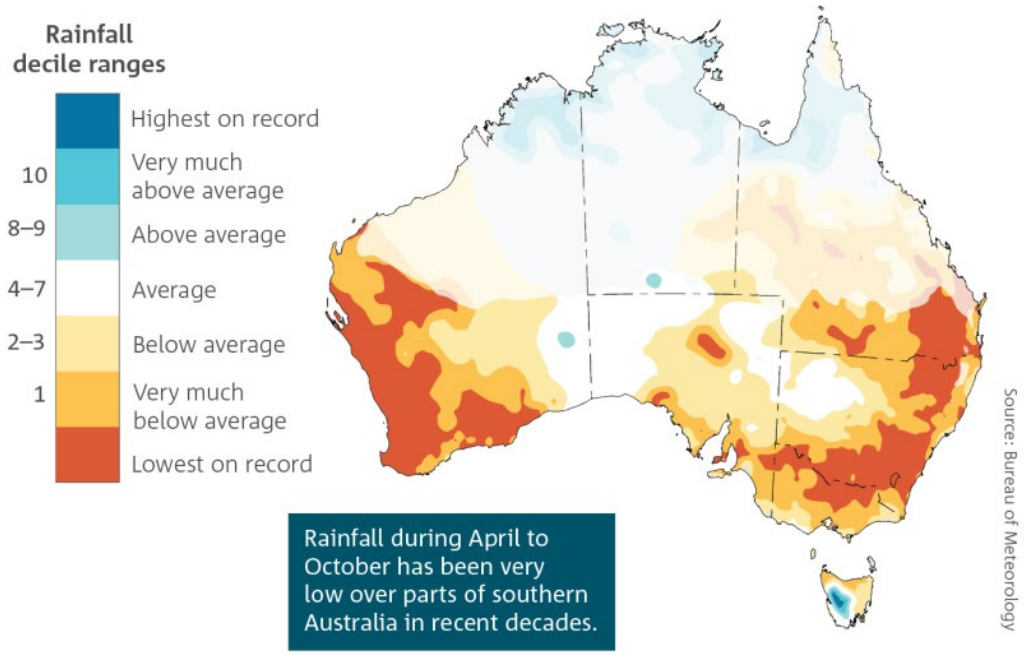

Figure 3: April to October rainfall deciles between 2000 and 2019 compared to the entire rainfall record from 1900 – 2019. Note recent wet years (2020, 2021, 2022) are not included. Source: http://www.bom.gov.au/state-of-the-climate/.

The large inter-annual rainfall variability has led to many regions across NSW experiencing prolonged meteorological droughts and severe floods. Four major multi-year droughts have occurred in NSW over the observational period (~1900 to present); The Federation Drought (1895-1903), World War II Drought (1939-1945), Millennium Drought (1997-2009) and the more recent 2017-2020 'Tinderbox' drought [10–13]. Multi-year droughts have devasting effects on urban and regional water supply, agriculture, and the broader economy [14]. However, the limited number of multi-year droughts within the relatively short instrumental record makes it difficult to assess the climate dynamics leading to drought and drought breaking rainfall in Australia. Additionally, the length of the instrumental rainfall record (generally post 1900, but longer in parts of southern Australia [15]) is insufficient to assess decadal to multi-decadal variability and the risk of multi-year droughts [16–20]. This constrains the development of robust water security policy and infrastructure to mitigate impacts of future droughts, as the worst possible drought due to natural climate variability may not be realistically represented in the instrumental record [21,22]. Similarly, the length of the flood history data extending back to historical records in the late 1800s limits the ability to determine the worst flood possible for different catchments. Widespread flooding across NSW often occurs in multi-year to decadal cluster periods, with the most notable large floods occurring between 1860-1890, 1940-1950s, 1970s, 2010-2012 and 2020-2022 [23].

Rainfall variability prior to the instrumental record can be inferred from palaeoclimate proxies sensitive to wet and dry conditions, including tree rings, coral cores, speleothems (cave deposits), lake sediments and ice cores Across the Northern Hemisphere, there is an extensive network of annual growth rings obtained from long-lived tree species that can be cross dated to provide local, high resolution (seasonal to annual), continuous and long (>500 years) rainfall proxies to understand past drought variability [24]. However, these types of records are spatially limited in Australia due to many native tree species not producing clear or annual rings (Figure 4) [25]. The majority of tree ring records in Australia are located in regions with strong seasonal climate influences, including Tasmania, southwest Australia and northwestern Australia, remote from the major urban and agricultural regions, and extend back ~400-600 years [11,25–28]. Coral cores also provide high resolution rainfall variability over the past ~400 years but are focussed in northern Australia [29,30]. Multiple lower resolution (> annual) local proxy records of hydroclimate, such as cave deposits (speleothems: annual to decadal) and lake sediments (decadal to centennial), have been developed from archives in the Australasian region. These preserve past hydroclimate variability over longer temporal periods (2000+ years) [31–33]. However, their reduced temporal resolution makes it difficult to determine the duration and frequency of past wet and dry epochs [22]. Remote high resolution palaeoclimate records that have climatological links to Australian climate conditions

(e.g., Antarctic ice cores, New Zealand tree rings and coral cores from the Pacific and Indian Oceans) have also been utilised to complement the limited number of local proxy records [11,21,26,28,34–37].

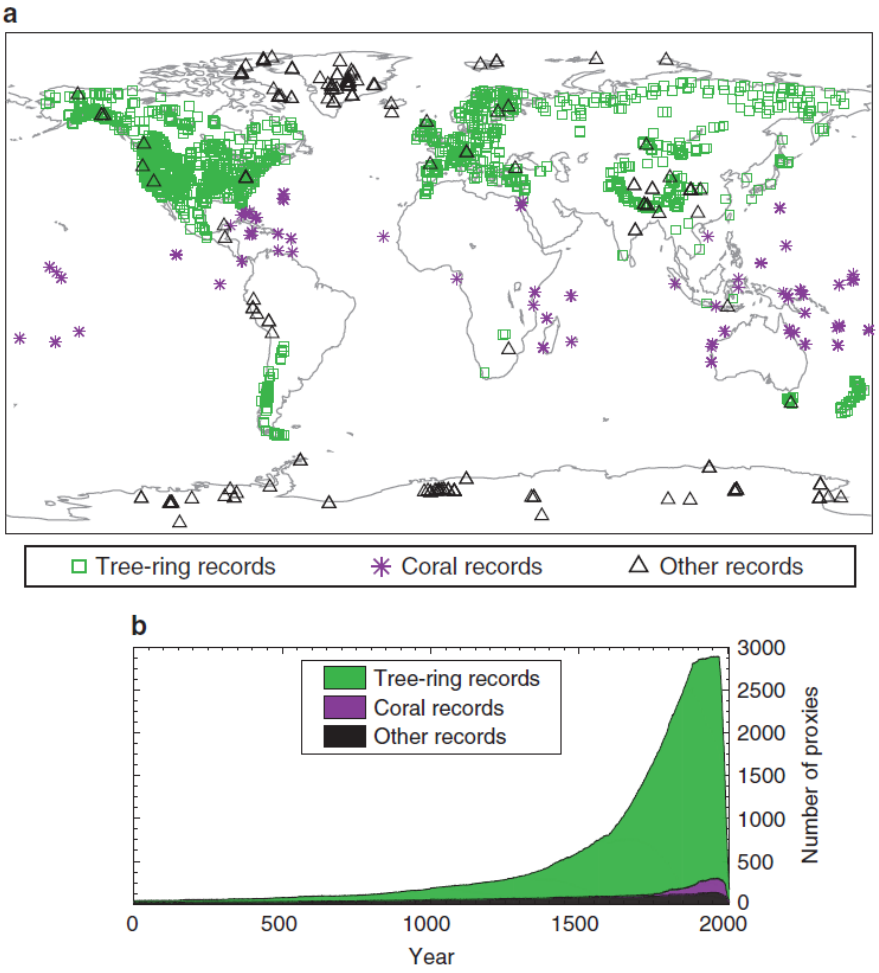

Figure 4: Location of high resolution (seasonal – annual resolution) hydroclimate (rainfall and/or temperature) proxies. Source: Steiger et al.[24]

A comparative study of wet and dry periods based on local and remote palaeoclimate records for eastern Australia indicates that rainfall variability over the relatively short instrumental era underestimates the full range of variability that has occurred over the past millennia. In particular, the instrumental record likely underestimates the duration and frequency of both wet and dry periods [21]. The proportion of dry years during the 1000s, 1100s and 1400s was greater than dry periods experienced in the 20th century (Figure 5), with multiple multi-decadal megadroughts suggested by four separate records; ice core records of atmospheric moisture transport [36,37], Wombeyan cave speleothems [17], and vegetation changes recorded in lake sediments from southern Queensland [31] and Victoria [32]. The proportion of wet years over the 1500s to 1800s is also greater than the wet years experienced in the 20th century [21]. These results highlight the need for continuous, multi-century (>500 years) records to capture both the dry and wet epochs over recent millennia to provide context to hydroclimate extremes that have occurred in the 20th and 21st centuries. Records that only extend back to the wetter centuries over the last 500-600 years (e.g., currently available tree rings) may underestimate the natural occurrence of dry periods [38].

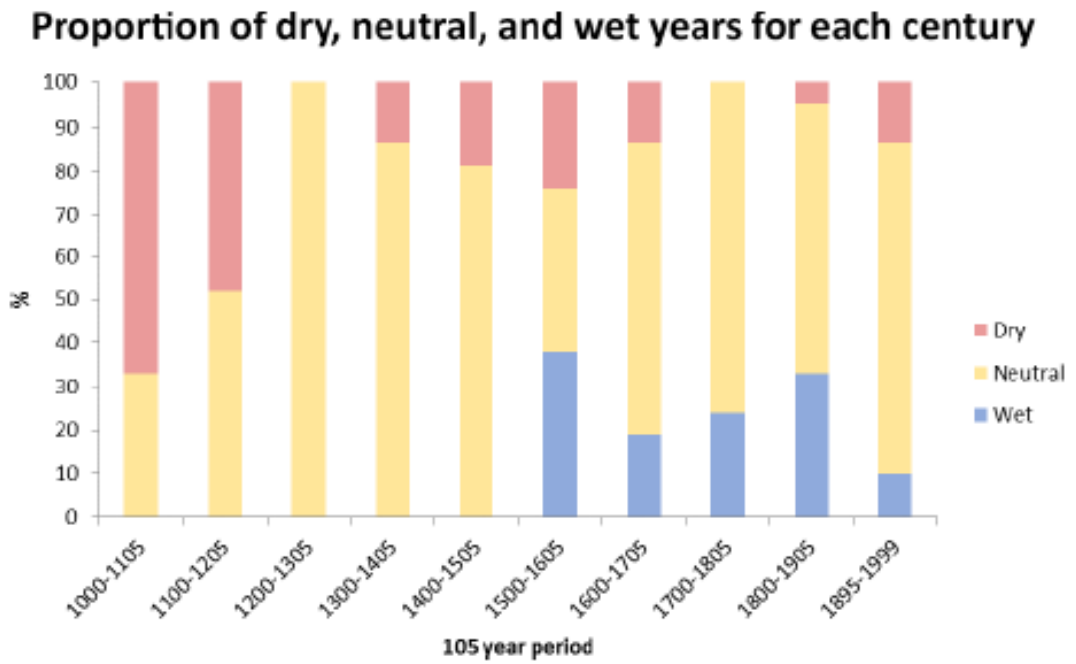

Figure 5: Proportion of dry, neutral, and wet years for each 105-year period between 1000 to 2000 CE. Source: Flack et al.[21]

3 Summary of weather and climate drivers

The weather and climate of NSW are influenced by the interaction between modes of climate variability over the Pacific, Indian and Southern Oceans across seasonal to multi-decadal time scales[5,39]. The phase of the climate variability modes shifts the probability of above or below average rainfall through changes in atmospheric circulation and weather systems that deliver rainfall to NSW (Figure 6). The compound influence of climate modes of variability on NSW rainfall is summarised in Section 3.2 and the dominant weather and climate drivers of NSW rainfall variability are summarised in Section 4.

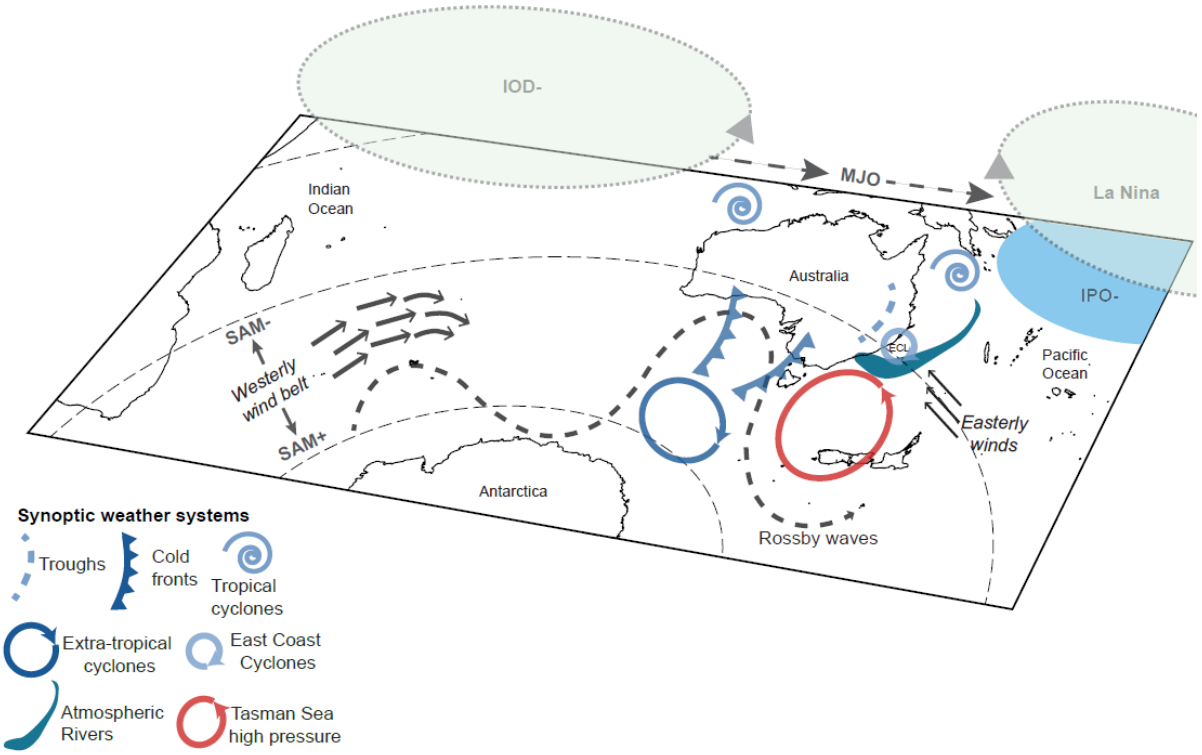

Figure 6: Schematic of synoptic-scale weather and modes of climate variability that are important for rainfall over NSW

NSW rainfall is influenced by a combination of factors across spatial and temporal scales, from synoptic weather and large-scale circulation to remote modes of climate variability. The frequency of synoptic weather systems that deliver rainfall to NSW are modulated by interactions between modes of climate variability. The rainfall influence associated with drivers also vary by season and region. For example, the influence of SAM shifts between winter and summer and IOD+ conditions have an opposing influence between inland and coastal NSW.

Over **coastal and northeast inland NSW**, surface onshore easterly winds increase moisture and leads to rainfall as the air parcel is uplifted over the Great Dividing Range. Weather and climate drivers that enhance the easterly wind strength and vertical uplift are associated with widespread rainfall (e.g. La Niña, SAM+, east coast lows, atmospheric rivers and Tasman Sea high blocking). This region receives most of its rainfall between November and March.

Over **southern inland NSW** enhanced westerly surface winds associated with cold fronts and extra-tropical cyclones during the cool season (May-October) are associated with increased rainfall through orographic uplift on the western side of the Great Dividing Range. These weather systems are more likely during SAM- conditions. This region receives most of its rainfall between May and October.

3.1 Modes of climate variability

This section summarises the modes of climate variability that influence NSW rainfall, including IPO, ENSO, IOD, SAM and MJO. A description of each driver, how they influence the probability of rainfall across NSW and datasets are provided for each mode of variability. The interaction between the modes of climate variability is summarised in Section 3.2.

3.1.1 Interdecadal Pacific Oscillation (IPO)

The IPO is a low-frequency (15-35 year) pattern of ocean-atmosphere variability of the tropical and extra-tropical Pacific Ocean. The IPO represents a significant mode of climate variability that drives changes in mean sea level pressure, temperature and rainfall across NSW and the MDB [19,23,40]. The IPO changes phase from positive (warm) to negative (cool) on a pseudo-decadal basis, however the underlying climatological mechanism/s that force a shift to another phase are not well understood [41]. The positive phase is characterised by above average sea surface temperature (SST) in the tropical Pacific and below average SST in the extra-tropical Pacific. Negative IPO is characterised by below average SST in the tropical Pacific and above average SST in the extra-tropical Pacific (Figure 7). Rainfall across NSW and the MDB is significantly lower during IPO positive years compared to IPO negative [19,42]. IPO also modulates the magnitude, frequency and impact of ENSO events on eastern Australian climate [19,23,40]. This results in multi-decadal periods of elevated flood (during IPO negative and La Niña) and drought (during IPO positive and El Niño) risk [19,23].

Over the instrumental record the IPO variability appears to be cyclical with similar length of time (~20-30 years) spent in positive and negative phases. However, an underlying internally generated climate process to cause this consistent decadal scale oscillation has not been identified [41]. Additionally, palaeoclimate reconstructions that span the Common Era (past ~2000 years) suggest that the length of time spent in each phase is significantly different [42]. IPO reconstructions from individual sources, including ice cores and tree rings demonstrate that the IPO is biased toward a neutral to positive state over the past 2000 years, while negative phases tend to be shorter (<7 years) and more infrequent (10-150 years between negative phases) [42–44]. This contrasts with the instrumental record where each phase has similar length and frequency [23,40,45]. This means that inferences around the impact of IPO behaviour on the variability of NSW rainfall from the observational record may not reflect the underlying variability that is possible [42]. As an example – if positive phases are more prevalent over the longer term, this means a drier than usual climate (where usual is defined based on the observational record) may be the longer-term normal for NSW because of the influence of positive IPO phases on rainfall variability through the modulation of ENSO influences on NSW. Conversely, it is currently unknown what impact anthropogenic climate change may have on IPO phase intensity, frequency or duration. If there is a change in IPO behaviour due to anthropogenic climate change, then there will be a resultant change in the modulation and frequency of ENSO events and their impacts on NSW rainfall.

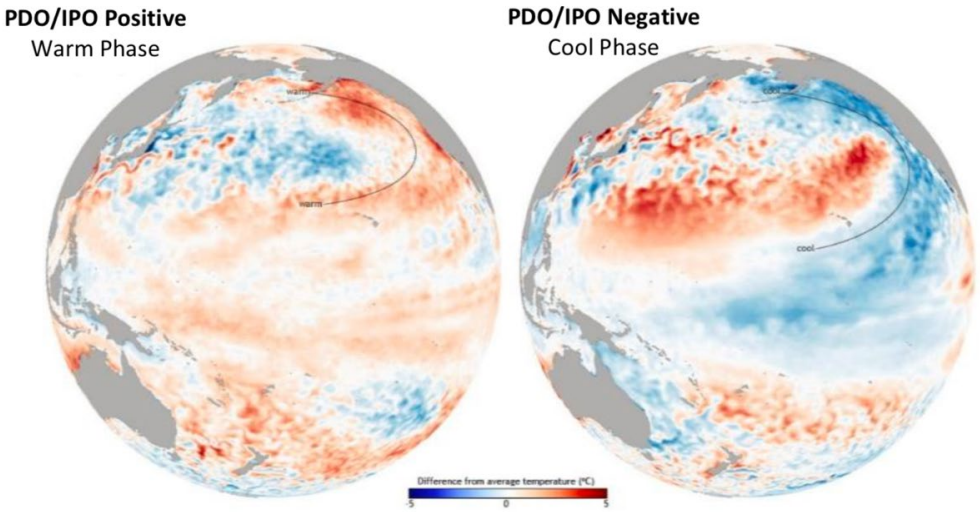

Figure 7: Sea surface temperature anomaly patterns for IPO positive and negative phases. Source: https://takvera.blogspot.com/2014/01/warming-may-spike-when-pacific-decadal.html.

3.1.1.1 Datasets

Observational period

Several different indices have been calculated from SST observations to represent IPO variability (also referred to as Pacific Decadal Oscillation (PDO) or Pacific Decadal Variability (PDV)). The primary difference between IPO and PDO indices is the spatial scale used to calculate the index; IPO covers a broader spatial scale over the Pacific, including extra-tropical Southern Pacific, while PDV only includes the North Pacific.

The two main indices used to characterise IPO variability are the 'Folland' [46] and Tripole Index [45]. Both indices are calculated by mathematically filtering the SST datasets to capture key spatial and temporal patterns in the data. The 'Folland' index extends back to 1856 and was used for IPO reconstructions in Vance et al [42] and Buckley et al [43] (Figure 8). Monthly, seasonal and annual filtered (11-year low pass filter) and unfiltered data is available by contacting Chris Folland or through the New Zealand government data service (seasonal and annual index between 1871 to 2016; https://data.mfe.govt.nz/table/89382-interdecadal-pacific-oscillation-18712016/).

The Tripole index [45] is calculated using SST data from three regions of the Pacific; northern Pacific, eastern/central tropical Pacific and southwest Pacific. Monthly IPO Tripole Index is available between 1854 and near present: https://psl.noaa.gov/data/timeseries/IPOTPI/

Palaeoclimate reconstructions

There are at least 16 published annual Pacific Decadal Variability reconstructions from various archives including tree rings, coral cores and ice cores [38,42,43]. Twelve of these reconstructions are summarised in Zhang et al[38] and include nine reconstructions that extend back 300-400 years from North Pacific tree rings (North America and east Asia sites) and coral cores from the South Pacific. An additional three reconstructions cover the past ~1000+ years and are sourced from tree rings in the North Pacific [47], the Law Dome ice core in East Antarctica [36] and a global multi-proxy [48]. Four more IPO reconstructions have been developed since the Zhang et al[38] review including 1) a trans-Pacific tree ring based reconstruction extending back to 1350 CE by Buckley et al[43] 2) a Pacific wide ice core based reconstruction extending back to 1450 CE by Porter et al [44], 3) an extended reconstruction covering the past 2000 years from the Law Dome ice core by Vance et al [42] and 4) a 400 year reconstruction using dust concentration in a Northern Greenland ice core[49].

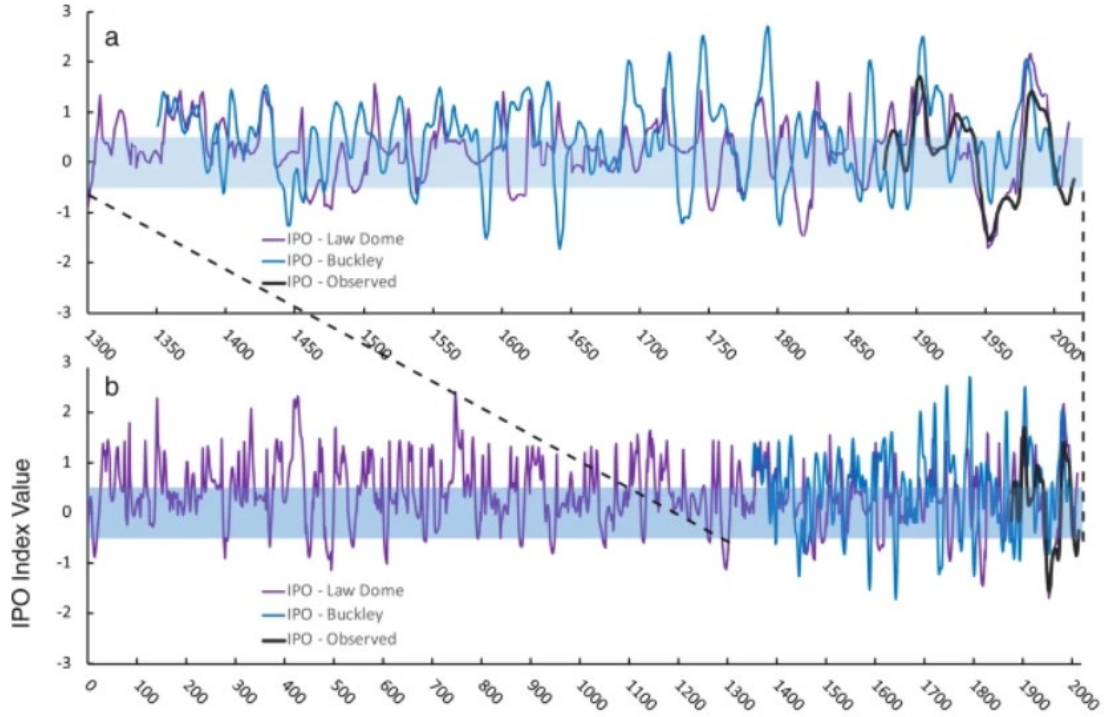

Figure 8: IPO timeseries over the past 2000 years. a) The extended Law Dome IPO reconstruction and Buckley et al.[43] IPO reconstruction from 1300 – 2011, and b) the past 2000 years. The black line is the observational IPO using the Folland index. Source: Vance et al[42]

Reconstruction datasets available on data centre portals include:

- D'Arrigo et al (2001), Pacific Decadal Oscillation Reconstruction: https://www.ncei.noaa.gov/access/paleo-search/study/6268
- MacDonald and Case (2005), Pacific Decadal Oscillation Reconstruction for the Past Millennium: https://www.ncei.noaa.gov/access/paleo-search/study/6338
- D'Arrigo, R. and R. Wilson (2006), Spring Pacific Decadal Oscillation Index Reconstruction: https://www.ncei.noaa.gov/access/paleo-search/study/6361
- Buckley et al. (2019), Interdecadal Pacific Oscillation reconstruction: https://link.springer.com/article/10.1007/s00382-019-04694-4
- Porter et al (2021), Interdecadal Pacific Oscillation Index 550 Year Reconstruction: https://www.ncei.noaa.gov/access/paleo-search/study/33092
- Vance et al (2022), A common Era reconstruction of the Interdecadal Pacific Oscillation form the Law Dome ice core, East Antarctica: https://doi.org/10.26179/vk1n-5t86

The Buckley et al[43] reconstruction is not available on public data portals but may be available through contacting the corresponding author.

3.1.2 El Niño-Southern Oscillation (ENSO)

ENSO is characterised by interannual variations (~3-7 year cycles) in SST across the tropical Pacific Ocean, causing global changes in atmospheric circulation and ocean currents [50–52]. Shifts in ocean and atmospheric circulation influence global wind and rainfall patterns, causing variability in extreme events such as droughts, floods, and tropical cyclone activity [19,23,40]. ENSO event onset occurs between April and September and events mature between October and March. The phases of ENSO represent the migration of the Walker Circulation, a thermally driven west-east zonal cell, across the Pacific Ocean (Figure 9). Under neutral conditions, the rising limb of the Walker circulation is positioned over Indonesia and the descending limb over the eastern Pacific Ocean. During La Niña conditions, the neutral phase circulation patterns are enhanced causing strengthened southeast trade winds and increased rainfall over eastern Australia. Conversely, El Niño conditions are characterised by weakened or reversed trade winds, decreasing rainfall in the western Pacific region as the rising limb of the walker circulation shifts eastward towards the central Pacific Ocean.

The stages of ENSO are determined using the atmospheric pressure and ocean SST anomaly datasets. The Southern Oscillation index (SOI) represents the shift in the Walker circulation based on the sea level pressure difference between Darwin and Tahiti. The oceanic indices represent the SST anomalies (SSTAs) over different regions of the eastern (Niño1+2, Niño3) and central tropical Pacific (i.e, Niño 3.4, Oceanic Nino Index, Niño4). El Niño events are characterised by negative SOI and positive SSTAs, while La Niña events are represented by positive SOI and negative SSTAs.

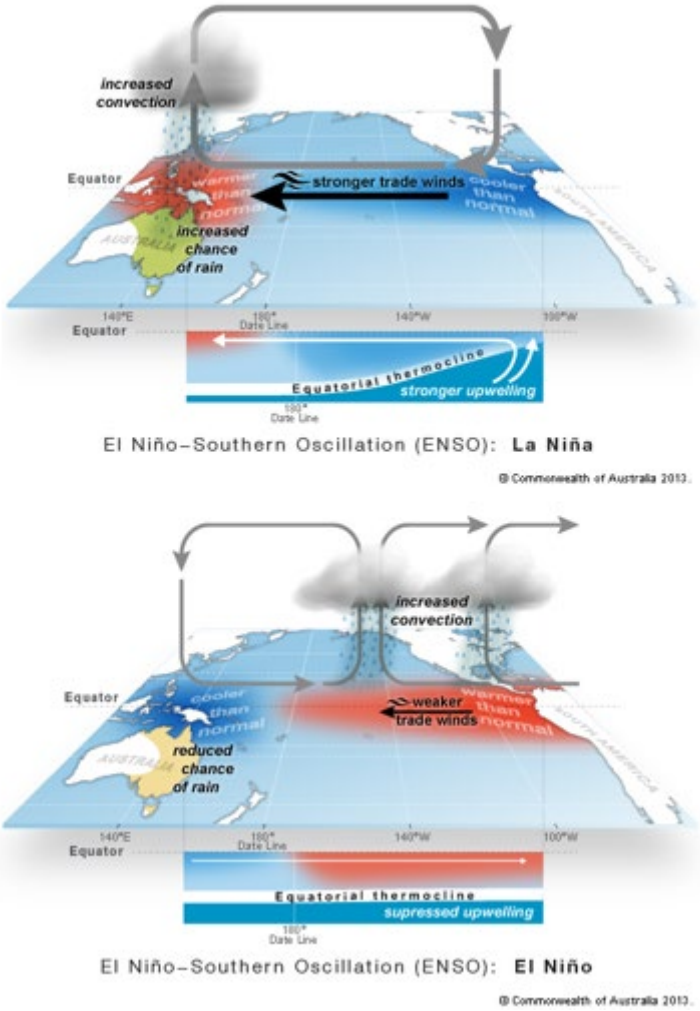

Figure 9: Schematic of the average Walker circulation pattern, Sea Surface Temperature and rainfall response during La Niña and El Niño events. Source: Bureau of Meteorology.

The influence of ENSO on NSW rainfall varies by season and region. ENSO has the strongest influence across most of NSW during winter and spring, however the influence on rainfall between June to October is only significant west of the Great Dividing Range 5,53. The lack of correlation over coastal NSW between June to October is due to the IOD opposing the influence of ENSO through shifts in the zonal (west to east) wind regime 53. During summer, the ENSO influence on rainfall is strongest along the NSW east coast and weak or non-significant across inland regions (including the Murray Darling Basin) 1,3,5. During Autumn, ENSO has limited influence on monthly rainfall, with significant correlation regions isolated to the northeast coast and parts of the south coast. There is also considerable multi-decadal variability in the relationship strength 19,23,40. The relationship between ENSO and NSW rainfall is stronger during periods of negative IPO (e.g., 1948-76) and weaker during positive phases (e.g., 1919-47) 19,23,40. This is due to negative IPO conditions favouring more intense and frequent La Niña's 23,54, which have a stronger relationship with rainfall across eastern Australia compared to El Niño conditions 55,56.

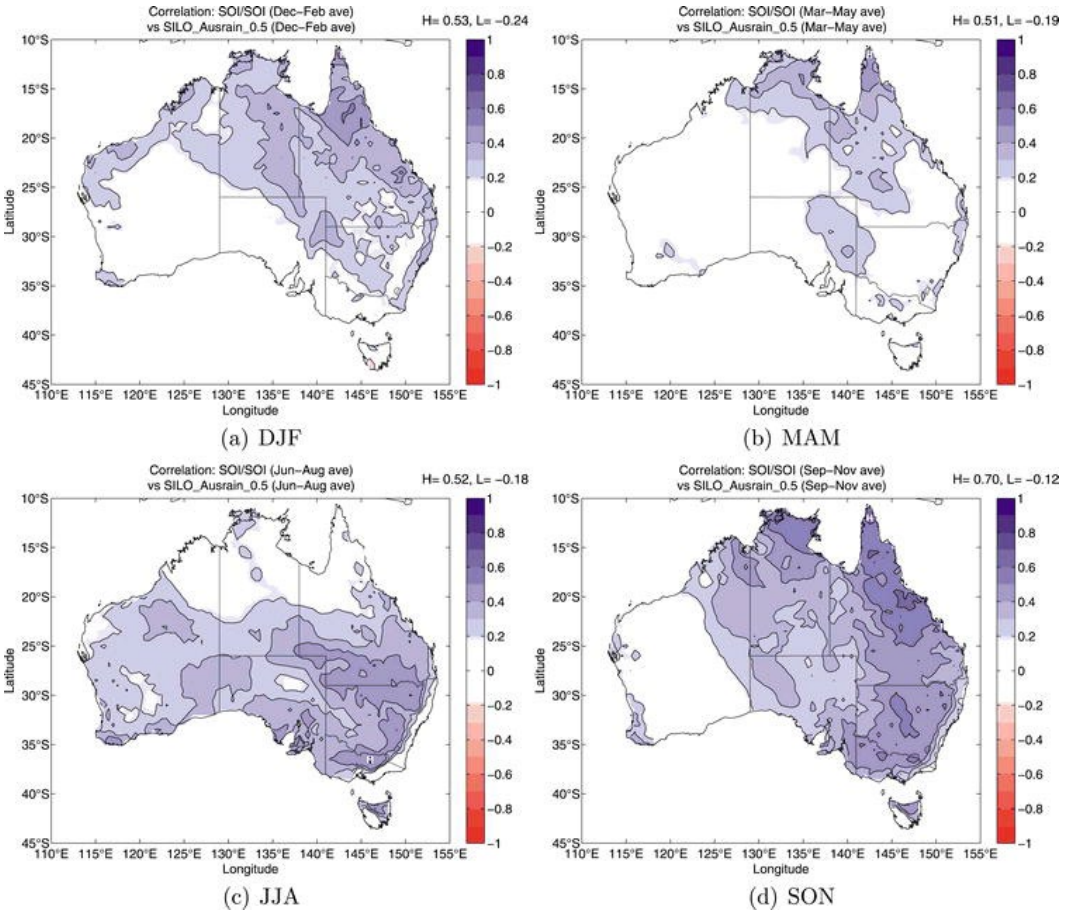

Figure 10: ENSO relationship with Australian rainfall. Correlation between Southern Oscillation Index and Australian rainfall for each season a) DJF - summer, b) MAM - autumn, c) JJA - winter, d) SON - spring. Only correlations significant at 95% level are shown. Data period: 1889 to 2006. Source: Risbey et al [5].

The relationship between the strength of an ENSO event and eastern Australian rainfall is also nonlinear. The relationship between La Niña strength and rainfall is relatively linear, with stronger or more intense La Niña events associated with increased rainfall conditions [55–57]. However, the strength of El Niño events is unrelated to the intensity of drying conditions [55,56]. For example, the strong El Niño events in 1982/83, 1997/98 and 2015/16 caused very different rainfall impacts across Australia [58]. During the 1982/83 event, eastern Australia experienced large rainfall deficits typical of El Niño conditions. However, the similar strength 1997/98 and 2015/16 El Niño events resulted in near average rainfall [58–60]. Some of these differences have been connected to the varying SSTA spatial characteristics of El Niño events [58]. The strongest SSTAs associated with eastern Pacific El Niño events are focussed off the South American coast, whereas central Pacific El Niño events peak around 150°W [60]. Unlike all El Niño events combined, the strength of central Pacific El Niño events are linearly related to rainfall anomalies across parts of inland and coastal NSW [61]. However, the sign of the anomaly is opposite depending on the season, with dry conditions experienced in the onset phase (April to September) and wet conditions during the mature phase (October to March) (Figure 11). During strong central Pacific El Niño events this reverse in rainfall anomaly patterns is associated with the wind regime over southeast Australia shifting from a dry westerly flow (August to October) to a moist easterly flow (January to March). These conditions are often associated with drought intensification prior to drought-breaking rainfall, for example the 2009/10 and 2019/20 seasons [61].

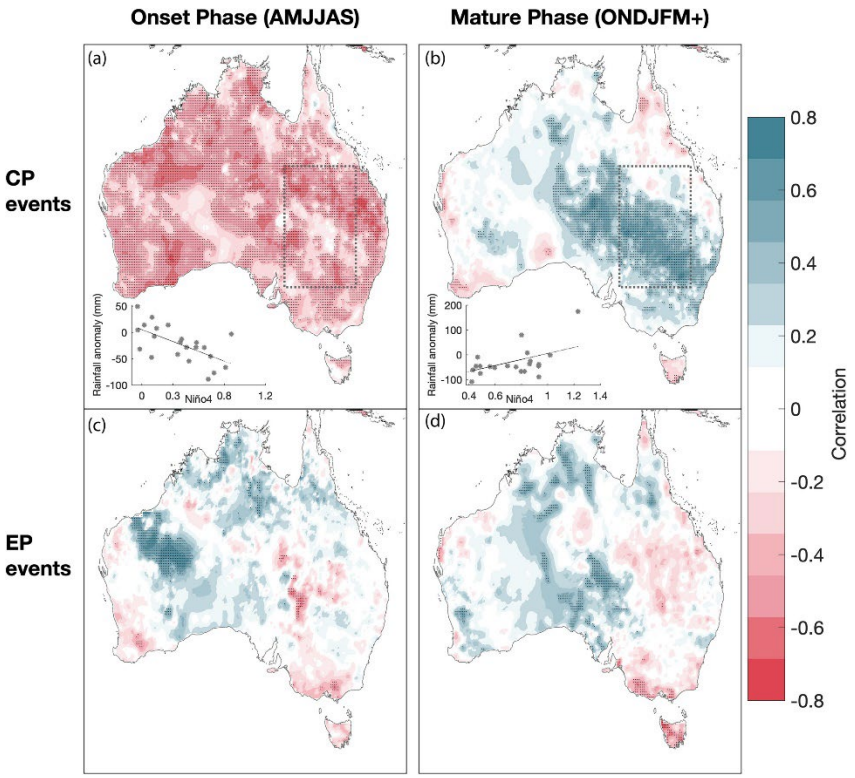

Figure 11: Pearson correlation coefficients between the Niño4 index during the onset phase and mature phase for Central Pacific El Niño events and Eastern Pacific El Niño events. Source: Freund et al[61]

3.1.2.1 Datasets

Observational period

Monthly and seasonal indicies can be downloaded from multiple data repositories including the Australian Bureau of Meteorology (SOI - http://www.bom.gov.au/climate/enso/soi/) and the United States of America National Center for Atmospheric Research (SST indicies - https://climatedataguide.ucar.edu/climate-data/nino-sst-indices-nino-12-3-34-4-oni-and-tni).

Historical and Palaeclimate reconstructions

Coral and tree ring records from the equatorial Pacific provide local insight into ENSO variability, however the number and length of these records are limited [62,63]. Remote proxies that have significant relationships to ENSO variability, such as North American tree rings [e.g. 50] and Antarctic ice cores [e.g. 64] provide additional insight into ENSO variability over the past 500-1000 years. Additionally, a recently collected ice core from East Antarctica (Mount Brown South) has strong correlations with ENSO over the past ~40 years [65] and has the potential to provide additional insight into ENSO variability over the past 1000 years once developed. Historical record (pre 1900) reconstructions have also been produced using observations contained within ship logbooks [66]. Table 1 summarises ENSO reconstructions available through the NOAA palaeoclimate data portal; https://www.ncei.noaa.gov/access/paleo-search/

Table 1: Selection of ENSO reconstructions available through the NOAA palaeoclimate data portal (ordered by year of publication)

Authors (Year), Dataset title	Data portal link
Stahle et al (1993), Southern Oscillation Index 275 Year Reconstruction	https://www.ncei.noaa.gov/access/paleo-search/study/16459
Cook et al (2005), Nino3 Index reconstruction of the Eastern Pacific Ocean from 1408 to 1978	https://www.ncei.noaa.gov/access/paleo-search/study/6250
Braganza et al. (2009), Multiproxy ENSO Reconstructions	https://www.ncei.noaa.gov/access/paleo-search/study/8409
McGregor et al. (2010), 350 Year Unified ENSO Proxy Reconstruction	https://www.ncei.noaa.gov/access/paleo-search/study/8732
Wilson et al (2010), Nino3.4 SST 460 year reconstructions	https://www.ncei.noaa.gov/access/paleo-search/study/11749
Li et al. (2011), 1,100 Year El Niño/Southern Oscillation Index Reconstruction	https://www.ncei.noaa.gov/access/paleo-search/study/11194
Yan et al. (2011), 2000 Year Precipitation-Based Southern Oscillation Index Reconstruction	https://www.ncei.noaa.gov/access/paleo-search/study/12203
Emile-Geay et al. (2012), Central Equatorial Pacific Nino3.4 850 Year SST Reconstruction	https://www.ncei.noaa.gov/access/paleo-search/study/13684
Li et al. (2013), 700 Year El Niño/Southern Oscillation Nino3.4 Index Reconstruction	https://www.ncei.noaa.gov/access/paleo-search/study/14632
Tierney et al (2015), PAGES Ocean2K 400 year Coral Data and Tropical SST Reconstructions (Eastern and Western Pacific Coral-Based SST reconstructions)	https://www.ncei.noaa.gov/access/paleo-search/study/17955
Dätwyler et al. (2019), Multiproxy El Nino-Southern Oscillation 1,000 Year Reconstructions	https://www.ncei.noaa.gov/access/paleo-search/study/25891
Freund et al (2019), Nino Cold Tongue and Nino Warm Pool Index 400 year reconstructions	https://www.ncei.noaa.gov/access/paleo-search/study/26270
Dätwyler et al. (2020), El Nino-Southern Oscillation Index 1,000 Year Reconstruction	https://www.ncei.noaa.gov/access/paleo-search/study/29050

3.1.3 Indian Ocean Dipole (IOD)

The IOD is a coupled ocean-atmosphere phenomenon in the equatorial Indian Ocean, characterised by a dipole pattern in anomalous SST between the eastern (90-110°E, 0°-10°S) and western (50°-70°E, 0°-10°S) Indian Ocean [67]. The intensity and phase of the IOD is represented by the Dipole Mode Index (DMI) using monthly SST datasets (e.g. HADISST1.1) and a climatology period of 1981-2010.

IOD activity is seasonally locked by the wind reversals associated with the Asian-Australian monsoons. Events usually develop during autumn (March-May) and peak between August-October before rapidly decaying in early summer with the onset of the Australian monsoon season [67,68]. This means that the effect of the IOD on NSW rainfall is generally only during winter and spring. Positive IOD (IOD+) events are characterised by anomalously low SSTs in the eastern tropical Indian Ocean off Sumatra, Indonesia and high SSTs in the western tropical Indian Ocean (Figure 12). These SST anomalies are connected to enhanced ocean upwelling along the Indonesian coast, strengthened surface easterly winds along the Equator, and enhanced ocean warming in the western tropical Indian Ocean [69]. The cool SSTs off Indonesia are associated with reduced atmospheric convection, leading to reduced tropical cyclone development in the region and below average winter and spring rainfall across Australia in a broad northwest to southeast band [39,70–75]. IOD+ events occur on average every 4 years over the observational record and there has been 11 IOD+ events since 1960 [76,77]. During negative IOD (IOD-) events, the equatorial upwelling reverses to the western Indian Ocean leading to cool SSTs off eastern Africa, enhanced surface westerly winds along the equator and warm SSTA off Indonesia [67,69]. The anomalously low SSTs in the western Indian Ocean reduces convection, leading to drought conditions across eastern Africa, while the warm SSTs in the eastern Indian Ocean increase convection and rainfall over western and south-east Australia [71,74,78]. Since 1960 there has been 12 IOD- events [77].

The strongest NSW rainfall influence associated with IOD variability is focussed over the southern inland NSW regional catchments along the Murray River during late winter and spring [5,13]. Along coastal NSW the influence of IOD on rainfall is not statistically significant, but the phase can counter the influence of the expected ENSO-rainfall relationship [5,53]. IOD+ leads to increased onshore flow over coastal NSW which increases the likelihood of rainfall and causes a breakdown in the relationship to ENSO in this region [53]. In contrast, IOD- leads to enhanced westerly winds which leads to subsidence and reduced rainfall over coastal NSW [53].

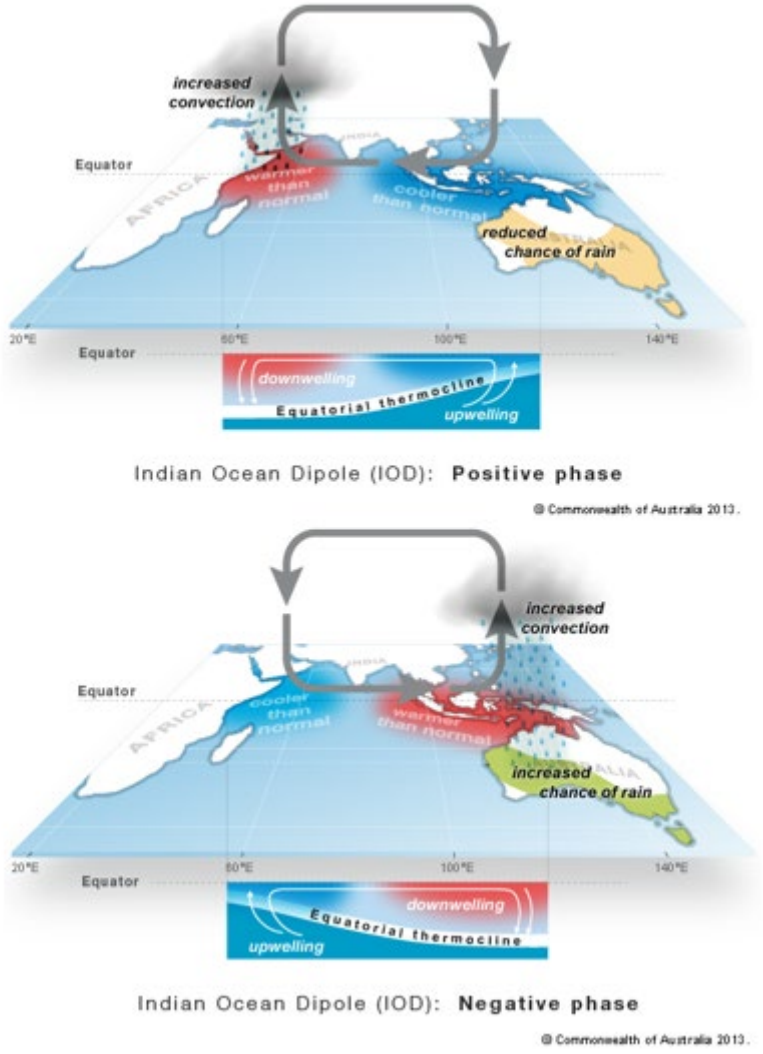

Figure 12: Schematic of the average Walker circulation pattern, Sea Surface Temperature and rainfall response during IOD positive and negative events. Source: Bureau of Meteorology.

3.1.3.1 Datasets

Observational period

The DMI monthly dataset from 1870 to present can be downloaded from https://psl.noaa.gov/gcos_wgsp/Timeseries/DMI/.

Palaeoclimate reconstructions

Coral core records from the western and eastern poles of the equatorial Indian Ocean have been used to reconstruct IOD variability. Datasets available on the NOAA palaeo portal (https://www.ncei.noaa.gov/access/paleo-search/) include:

- Abram et al (2015), Mentawai – d18O Data and DMI Reconstruction: https://www.ncei.noaa.gov/access/paleo-search/study/8607
- Tierney et al (2015), PAGES Ocean2K 400 year Coral Data and Tropical SST Reconstructions (Indian Ocean Coral-Based SST reconstruction): https://www.ncei.noaa.gov/access/paleo-search/study/17955
- Abram et al (2020), Southern Mentawai Islands d18O and d13C Data and Indian Ocean Dipole reconstruction over the last millennium: https://www.ncei.noaa.gov/access/paleo-search/study/28451

3.1.4 Southern Annular Mode (SAM)

The SAM explains most of the atmospheric variability (~35% variance) in the Southern Hemisphere. It describes the north-south (meridional) movement of the circumpolar westerly wind belt in the mid-latitudes of the Southern Ocean (e.g. to the south of Australia) and is related to the frequency and position of the moisture bearing cyclonic storms and moisture blocking high pressure systems that occur to the south of Australia (Figure 13a) [79,80]. This relatively simplistic explanation of SAM becomes more complex on the daily to seasonal timescales important for rainfall variability across NSW. The structure of SAM is typically described as zonally symmetric on an annual timescale, meaning that the westerly wind belt is assumed to be in essentially the same latitude position and circular in structure across all the Southern Ocean, as it appears in Figure 13a. However, the SAM is a high frequency climate mode which shifts between positive and negative phases on a weekly to monthly timescale and the reality of how the SAM affects Australian weather at the daily, monthly and seasonal timescales is related to the position of weather systems within the westerly wind belt. At these shorter timescales the structure of SAM is asymmetric (not circular), especially during spring and summer. This is because of the interaction between the phase of SAM and the daily position and intensity of low-pressure and high pressure systems in the southern mid-latitudes [79,81,82]. This asymmetry is important to NSW rainfall variability because it reflects the synoptic weather scale processes that are associated with rainfall extremes over NSW [3,82,83]. For example, the variability in the location of low and high pressure systems during positive SAM conditions influences where intense rainfall or dry conditions occur across NSW [3,82].

Since the mid-1970s, there has been a significant trend toward the positive phase of SAM during summer (Figure 13b) which has been attributed to the interaction between ozone hole depletion and greenhouse gas emissions [84,85]. However, since 2000 this trend has stabilised with the continued recovery of the ozone hole [84]. Increasing greenhouse gases and associated increased global temperatures are expected to force positive SAM conditions year-round through the expansion of the Hadley Cell [84,86].

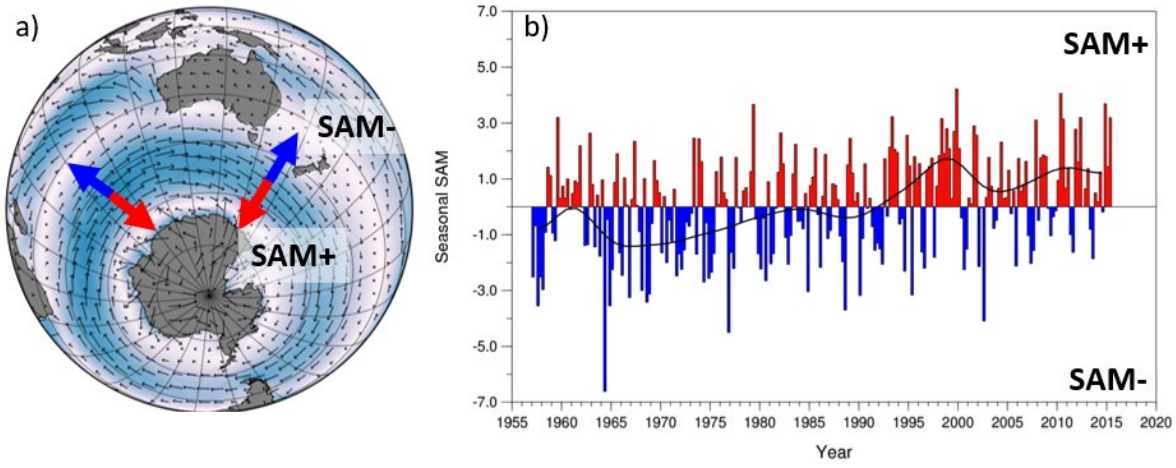

Figure 13: Southern Annular Mode. a) Annual average surface winds in the Southern Hemisphere showing polar easterlies, the mid-latitude westerly wind belt in the Southern Ocean to the north of Antarctica, and southeast trade winds along the eastern Australian coastline. Variability in the equatorward expansion and poleward contraction of the mid-latitude westerly wind belt (indicated by blue and red arrows) is characterised by the SAM. Figure created using ERA5[87] reanalysis surface winds (10m). b) Seasonal Marshall SAM index. Source: https://climatedataguide.ucar.edu/climate-data/marshall-southern-annular-mode-sam-index-station-based

The positive phase of SAM (SAM+) is associated with the general contraction of the circumpolar mid-latitude westerly wind belt poleward, resulting in stronger than average westerly winds over the high latitudes (55-70°S) and weaker westerly winds in the mid-latitudes (35-55°S) [80]. However, the asymmetry noted above affects the influence of SAM+ on daily to weekly synoptic weather patterns in the Australasian region, because the poleward contraction doesn't manifest as a perfectly circular atmospheric pattern. Instead, what is generally observed is an asymmetric contraction and intensification of mid-latitude westerly wind belt and a poleward shift in subtropical high-pressure systems over southern Australia [82,88]. The rainfall influence over NSW due to the poleward shift in high pressure over southern Australia (compared to seasonal climatological conditions)

varies based on the season, region and asymmetric structure of SAM+ conditions [3,5,82,89,90]. Specific to NSW, during winter, the poleward shift in high-pressure systems over southern Australia generally results in decreased chance of rainfall over southern NSW (due to the reduction in rain bearing cold fronts from the mid-latitudes) and conversely an increased chance of rainfall over northern and eastern NSW (due to increased moist onshore winds) [5,89]. In summer, the poleward shift in the subtropical high-pressure systems results in increased chance of rainfall across all of NSW and the MDB due to the high-pressure system in the Tasman Sea (part of the seasonal asymmetry described above) strengthening the moist easterly onshore flow [89]. Thus, the asymmetric contraction of the westerly wind belt in the Australian region results in varied precipitation anomalies across southern Australia (including NSW) during SAM+ conditions[3,82], and the complex patterns that result from the asymmetry need to be taken into account when applying the SAM phase to current or expected rainfall conditions for NSW.

The negative phase of SAM (SAM-) is characterised by higher pressures over Antarctica as the mid-latitude jet and low pressure 'storm belt' moves more to the north. This leads to increased frontal and extratropical cyclone activity over southern Australia [7,83,89]. The expansion of the westerly wind belt maintains a symmetric structure, in contrast to SAM+ conditions. This means there is a more consistent precipitation pattern across southern Australia, with less of the regional complexity that results from SAM+ conditions [82]. However, the precipitation influence of increased frontal activity across southern Australia during SAM- conditions is dependent on the season, and varies for different regions of NSW. During autumn and winter, SAM- conditions are associated with increased rain bearing cold fronts and extratropical cyclones making landfall across southern Australia leading to wetter than average conditions over southern NSW [89,91]. Over northeast NSW, the increased frontal activity shifts the wind regime to dry westerly offshore flow reducing the chance of rainfall [89]. During late spring and summer, the seasonal poleward shift in the mean location of the subtropical high-pressure belt and mid-latitude westerly wind belt changes the response of NSW rainfall to SAM- conditions. An equatorward expansion of frontal activity in late spring and summer causes dry and hot extremes across much of southern and eastern Australia, due to less moisture from easterly onshore winds [92]. The frontal activity also provides a mechanism to drive hot and dry air from the interior to southeast coastal and alpine regions of NSW and Victoria [93,94].

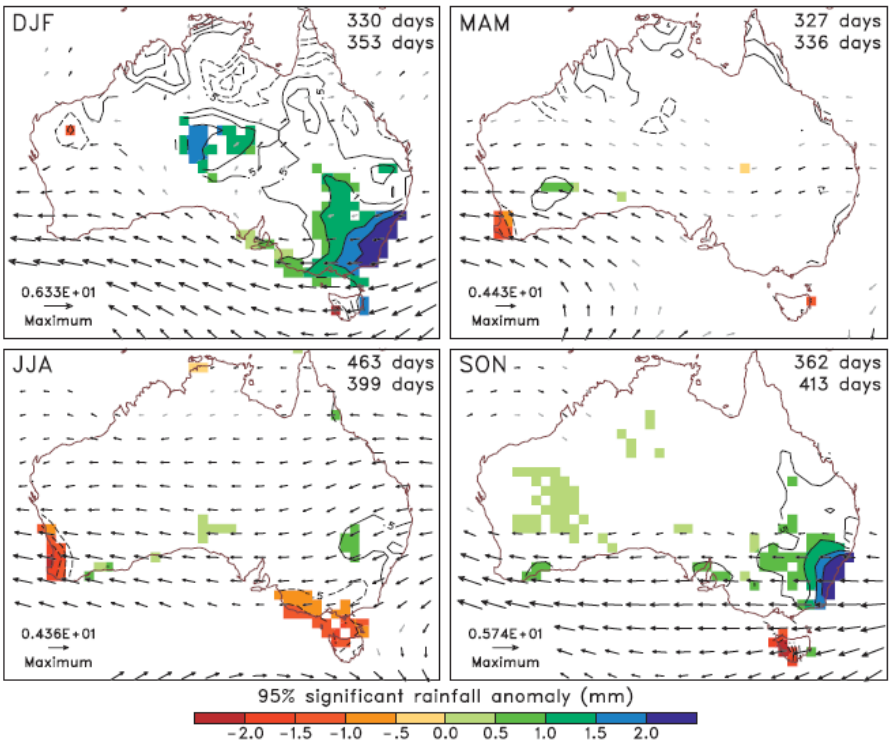

Figure 14: SAM influence on Australian daily rainfall. Composite daily rainfall (shaded) and 850-hPa wind (vectors) difference between positive and negative SAM (SAM+ minus SAM-) for each austral season. The number of days in the positive and negative phases of the SAM are listed in the upper right of each panel. The shading is only provided where the composite daily anomalies are significantly different from zero at the 95% level. Source: Hendon et al.[89]

3.1.4.1 Datasets

Observational period

The seasonal Marshall SAM index is available from https://climatedataguide.ucar.edu/climate-data/marshall-southern-annular-mode-sam-index-station-based

Palaeoclimate reconstructions

Multiple studies have reconstructed SAM using a combination of Southern Hemisphere tree rings and Antarctic ice cores (e.g. refs). Reconstruction datasets available on data portals include:

- Villalba et al (2012), Southern Annular Mode (SAM) Index 600 Year Tree Ring Reconstruction: https://www.ncei.noaa.gov/access/paleo-search/study/13673
- Abram et al (2014), Southern Annular Mode 1000 Year Reconstruction: https://www.ncei.noaa.gov/access/paleo-search/study/16197
- Dätwyler et al (2017), Southern Annular Mode 1,000 Year Reconstructions: https://www.ncei.noaa.gov/access/paleo-search/study/23130
- King et al (2023), Trends and Variability in the Southern Annular Mode over the Common Era: https://zenodo.org/record/7643732

3.1.5 Madden-Julian Oscillation (MJO)

The MJO is characterised by an eastward propagating cluster of tropical convection across the Indo-Pacific Ocean that interacts with the Walker and Hadley circulations [95,96]. It represents the dominant intra-seasonal (30-60 days) variability in the tropical atmosphere [97], and influences tropical and extratropical rainfall across Australia [98,99]. The clustering and propagation of the tropical convection is described by eight different phases using the real-time multivariate MJO index which is based mathematical functions that reveal key patterns in relevant climate variables including 850hpa zonal wind, 200hpa zonal wind and satellite observed outgoing longwave radiation (OLR) over the equatorial region [100].

The rainfall influence is strongest over northern Australia (up to 75% increased chance of rainfall) where the clustering of convection produces periods of enhanced or diminished convection [99]. MJO also indirectly influences rainfall across subtropical and temperate eastern Australia through tropical-subtropical circulation teleconnections (e.g. Rossby waves) and interactions with ENSO [98,99]. The extratropical influence of MJO on rainfall is strongest in winter and spring, with reduced chance of rainfall over inland NSW and the MDB during phase 3 and increased chance in phase 5 [98]. Phase 3 is associated with a stationary high geopotential height anomaly (anomalous high pressure) over southeast Australia which supresses convection and rainfall [99]. In contrast, phase 5 is associated with a low geopotential height anomaly (anomalous low pressure) over southeast Australia which enhances convection and rainfall [99]. MJO variability is also significantly correlated with rainfall over parts of the coastal NSW between Autumn and Spring, with increased chance of rainfall in phase 4 (autumn and winter; majority of eastern seaboard), phase 5 (autumn; majority of eastern seaboard) and phase 6 (spring; south coast). Phase 8 is associated with decreased chance of rainfall over both coastal and inland parts of NSW in autumn [98,99]. The duration of phase 5 and 6, which reflect an active MJO over northern Australia, has been observed to increase since 1974 [101].

3.1.5.1 Datasets

The real-time multivariate MJO index is available from 1975 to present on the Australian Bureau of Meteorology website: http://www.bom.gov.au/climate/mjo/. Other indices representing MJO variability are also available here: https://psl.noaa.gov/mjo/mjoindex/

The high frequency of MJO variability (daily to weekly variability) makes it difficult to reconstruct using palaeoclimate archives. The only record of an MJO signal in a natural archive is in a Giant Clam Shell from northern South China Sea [102]. This clam shell only covered a two-year period from January 2012 to December 2013, but the findings indicated that fossil shells from different geologic times could provide insight into MJO variability.

3.2 Compound influence of modes of variability on NSW rainfall

The phase of the IPO modulates the frequency and intensity of ENSO and SAM events, with negative IPO favouring increased frequency and intensity of La Niña events and SAM+ conditions [23,103]. IPO also influences the strength of the relationship between ENSO and IOD to NSW rainfall (strong during IPO negative, weak during IPO positive) [e.g. 40,104].

The seasonal-interannual interaction between ENSO, IOD, SAM and MJO phases can amplify or diminish the associated climate impacts across NSW [5,93]. ENSO and IOD events frequently co-occur during winter and spring, amplifying the rainfall anomalies over Australia [70,105]. The co-occurrence of in phase ENSO and IOD events in spring amplify the rainfall relationship expected with ENSO and IOD. For example, El Niño and IOD+ amplify below average rainfall conditions over southern inland NSW while La Niña and IOD- or neutral conditions lead to above average rainfall over most of NSW [13]. The co-occurrence of opposing ENSO and IOD phases (i.e. El Niño and IOD- / La Niña and IOD+) happen very infrequently in the observational record, however the phase of IOD appears to overpower the expected ENSO influence on rainfall. During late winter and spring, La Niña and IOD+ have co-occurred twice in 2007 and 2011 while the combination of El Niño and IOD- has only occurred in 1993. July to October rainfall over inland NSW in 2007 and 2011 were below average despite La Niña conditions, indicating the counter influence of IOD+ conditions [53,106]. The IOD- conditions in spring 1993 also appear to dominate the rainfall signal over El Niño, with above average rainfall across inland NSW and below average rainfall over coastal NSW between July – October [53,106]. IOD and ENSO are also strongly correlated in spring which makes it difficult to fully separate the impacts of the individual drivers [5,53].

When neither La Niña nor IOD- occurs over consecutive years there is an increase in the likelihood of multi-year droughts across southeast Australia, due to unfavourable atmospheric conditions for widespread rainfall reducing the chance of drought breaking rainfall [13]. The influence of ENSO and IOD on NSW rainfall can also be modulated by the phase of the MJO [107]. The west-east location of MJO convective activity can supersede the influence of ENSO and/or IOD phase conditions on rainfall. For example, despite La Niña and IOD- conditions in spring 2020, much of NSW recorded below average rainfall due to the MJO convective activity stalling in the central Indian Ocean which suppressed convection and rainfall over eastern Australia [107].

The interaction between ENSO and SAM phases also influences the individual impact of both climate modes on NSW rainfall [108,109]. The atmospheric circulation anomalies and associated surface weather conditions related with the different phases of each mode of variability amplify each other when they are in phase (e.g. La Niña/SAM+ or El Niño/SAM-) and counteract each other when phases oppose (e.g La Niña/SAM- or El Niño/SAM+) [79,110]. During spring and summer, the co-occurrence of La Niña/SAM+ conditions amplify the above average rainfall conditions over NSW associated with both modes of climate variability and increases the chance of atmospheric high-pressure blocking in the Tasman Sea [5,82]. These conditions increase the chance of drought breaking rainfall and flood hazard over NSW (e.g., 2010-11 spring-summer) due to favourable surface (i.e., moist easterly winds) and upper-level (i.e., trough or low) circulation conditions that support widespread convection and rainfall [1,3,111,112].

Dry conditions and fire hazard across NSW significantly increases during the co-occurrence of fire promoting phases of ENSO, SAM and/or IOD in spring and early summer [93], including; El Niño/IOD+, El Niño/SAM- and IOD+/SAM-. The atmospheric circulation anomalies associated with the combination of these modes of variability leads to increased frontal activity across southern Australia that drives hot and dry air from the interior of Australia towards the east coast [93,113]. El Niño and SAM- conditions have the strongest influence on fire danger over northern/central NSW, while IOD+ influence is strongest over southern inland NSW [93].

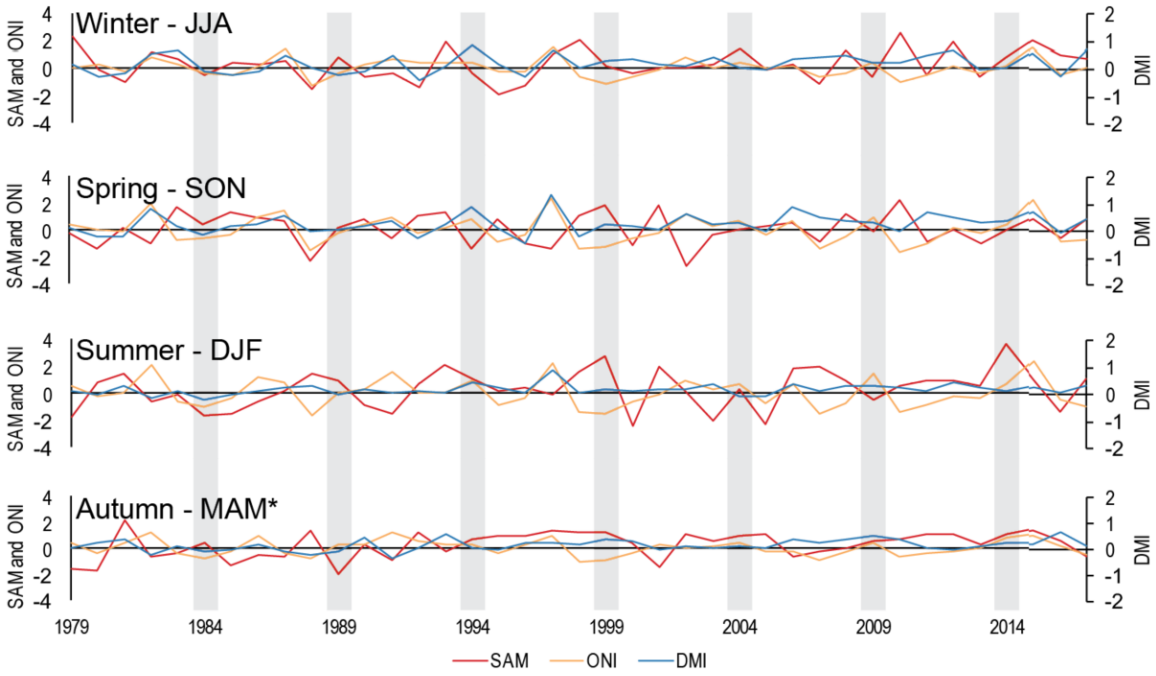

Figure 15: Seasonal average index for Southern Annular Mode (SAM) using the Marshall Index, Oceanic Niño Index (ONI) representing El Niño Southern Oscillation and Dipole Mode Index (DMI) representing Indian ocean Dipole. Year corresponds to December year. *note the MAM plot is year + 1 (e.g. MAM 2009 represents the period March-May 2010). Adapted from Udy et al.[82]

3.3 Summary of synoptic-scale weather systems important for NSW rainfall

The key synoptic scale weather systems important for NSW rainfall include east coast cyclones (including east coast lows), cold fronts, atmospheric rivers and Tasman Sea stationary high pressure systems (Figure 6). The frequency of these weather systems can be influenced by the modes of climate variability discussed in Section 3.1 Each of these weather systems are discussed in more detail below.

3.3.1 East Coast Cyclones (ECCs)

East coast cyclones (ECCs) are low pressure systems that impact the eastern seaboard of Australia, mainly between southern Queensland and eastern Victoria. ECCs are associated with widespread and intense rainfall over eastern NSW, often providing both drought breaking and flood-producing rainfall [6,8,114–116]. They can occur any time of year but have increased frequency between late autumn and early spring [115,116]. The inter-annual variability of ECCs is poorly understood with conflicting findings in the literature. Several studies have found partial modulation of the frequency of ECCs to be related to ENSO. However, the phase of ENSO that modulates ECC frequency is not consistent, with increased storm numbers observed in both La Niña and El Niño conditions [115–117]. Conversely, other studies have found no statistically significant relationships between ECC frequency and large-scale modes of climate variability [8,114].

These inconsistencies are likely related to the multiple 'sub-types' of ECCs that occur, as well as differences in how ECC classification/thresholds are applied in different studies. ECC sub-types include: 1) inland troughs; 2) easterly troughs; 3) frontal lows; 4) westerlies; 5) ex-tropical cyclones; and 6) rapidly intensified lows [6,116,117]. A recent clustering typology of ECCs found that the interannual variability of ECCs is sensitive to the 'sub-type' of cyclone and season [115]. Gray et al.[115] categorised six spatially independent cyclone types and classified them based on the location where they formed (coastal – C1,C2,C3, continental – C4,C5 and tropical – C6). The frequency of all six clusters were related to both ENSO and SAM variability in at least one season [115]. Four clusters (C2, C3, C5 and C6) displayed increased summer frequency during La Niña conditions, while the other two clusters (C1 and C4) were more likely during central Pacific El Niño conditions. Most clusters were more likely during SAM+ conditions across all seasons, except for winter frequency of C1 and C3 and summer frequency of C3 and C5 increasing during SAM- conditions. All six clusters are associated with increased rainfall

across parts of NSW; with the focus region varying between the types based on the cyclone origin [115]. ECCs originating off the northeast coast (C3) or the tropics (C6) mostly impact the northeast NSW region while storms originating off the central NSW coast (C2) impact the entire NSW coast and western slopes of the Great Dividing Range. ECCs originating over western NSW (C5) and southeast Australia (C4) result in widespread rainfall across NSW (strongest rainfall signal south of Sydney) and southern NSW respectively (Figure 16).

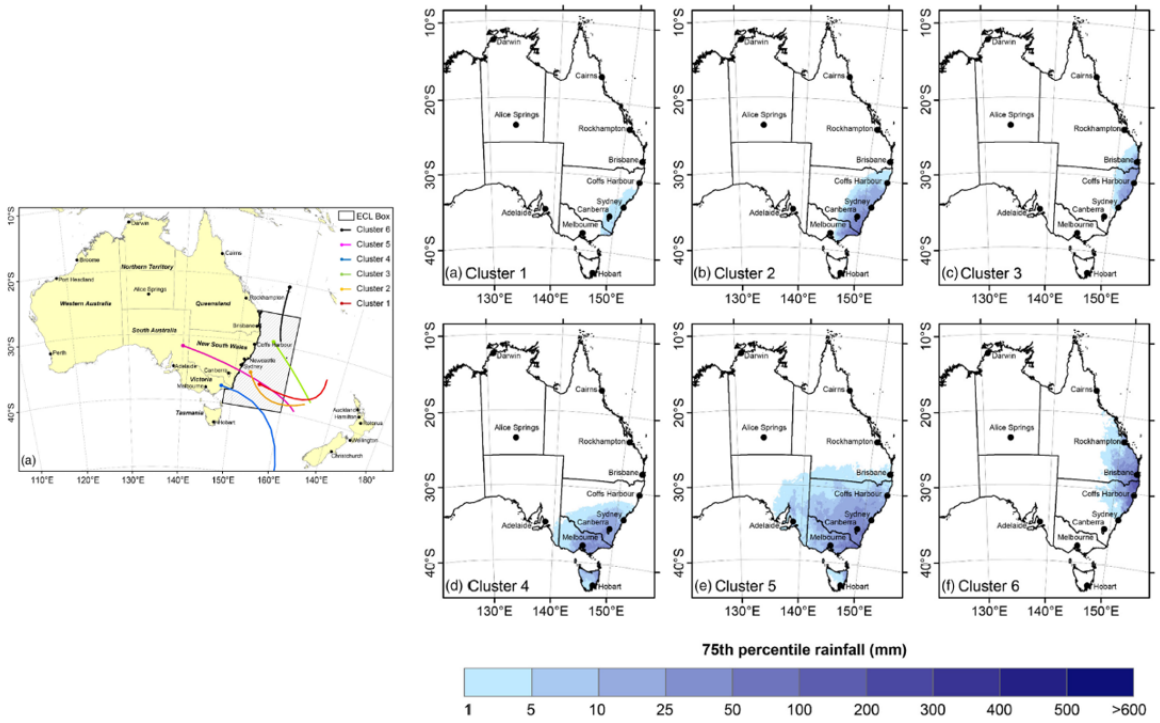

Figure 16: East Coast Cyclone sub-types. Left – cyclone clusters tracks. Right – 75th percentile rainfall. Source: Gray et al.[115]

Other ECC studies focus on a particular sub-type of cyclone, known as East Coast Lows (ECLs). ECLs are intense low-pressure systems with closed cyclonic circulation at the surface which form and often rapidly intensify near the eastern Australian coastline [6,8]. The criteria used to distinguish ECLs from other ECCs varies substantially between studies, with some studies using meteorological parameters while others use associated impacts (i.e. only considering extreme events with threats to life / property). Regardless of criteria used to define ECLs, they are associated with heavy rainfall across eastern NSW. For example, ECLs were identified as the dominant synoptic driver of 40% of widespread heavy rainfall over coastal NSW [8] and 60% of the largest inflow events into Sydney water supply dams [118].

3.3.1.1 Datasets

Refer to Gray et al [119] for detailed description of east coast cyclone / east coast low datasets available for eastern Australia.

3.3.2 Extra-tropical cyclones and cold fronts

Extratropical cyclones and their associated features, including atmospheric fronts and warm conveyer belts, are a major contributor to rainfall variability and extremes in the mid-latitudes [7,120]. Extratropical cyclones are large low-pressure systems that develop in the mid-latitudes (35°-55°S) along frontal zones separating cold and warm air masses. An atmospheric front, which refers to the interface between air masses of different thermal characteristics, can be classified as cold, warm, or occluded. The interaction between warm and cold air masses results in the uplift of airmasses and precipitation [121]. Extra-tropical cyclones and cold fronts move from west to east across southern Australia. Extra-tropical cyclones are associated with increased daily rainfall across NSW, with the strongest influence over the southwest region [7,122]. Cold front days are also associated with increased daily rainfall across inland NSW west of the Great Dividing Range [7]. Over the coastal regions, cold front days are associated with below average daily rainfall over northeast NSW and average conditions along the southern coast due to descending air reducing convection and chance of rainfall [7,53].

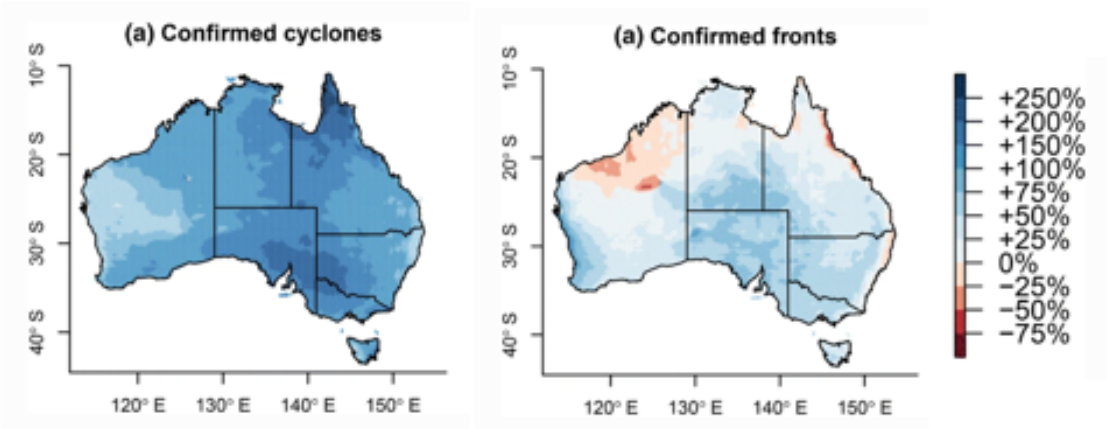

Figure 17: Annual percentage difference between average rainfall recorded with a cyclone or cold front, compared to the average daily rainfall across all day (1979-2015). Source: Pepler et al.[7]

3.3.2.1 Datasets

The weather typing datasets used in Pepler et al.[7,123] are an output of the Victorian Water and Climate Initiative and available for research purposes by contacting the authors.

Extratropical cyclones and fronts impacting southeast Australia are represented within SOM3 and SOM7 in Udy et al. [82]. The daily synoptic typing dataset from January 1979 to October 2018 can be downloaded from the Australian Antarctic Data Centre:
https://data.aad.gov.au/metadata/AAS_4537_z500_SynopticTyping_SouthernIndianOcean

3.3.3 Atmospheric rivers

An atmospheric river describes a type of weather pattern that transports warm moist air from the tropics to higher latitudes [124]. An atmospheric river is characterised by a long, narrow, and transient corridor of strong horizontal water vapour transport, and is typically located ahead of the cold front region in extratropical cyclones [124,125]. Spatial overlap between warm conveyer belts and atmospheric rivers is common. However, a key difference between the two phenomena is the direction of the moisture transport. Warm conveyer belts are associated with strong vertical movement from the boundary layer to the upper troposphere while atmospheric rivers are linked to strong horizontal movement of moisture usually confined to the lower troposphere [124]. Investigating the dynamics and impacts of atmospheric rivers in Australia is a developing area of research with Reid et al.[125] undertaking the first dedicated study.

Globally, atmospheric rivers are associated with extreme precipitation and floods [126–131]. In Australia, atmospheric rivers are associated with up to 30-50% of total rainfall and 15% of extreme rainfall days [125]. Atmospheric rivers in the Australian region are most frequent in summer and autumn, and least frequent in spring. The annual frequency of atmospheric rivers is high ranging from 350 to 540 events per year between 1980 – 2019 [125]. The strongest influence occurs over subtropical eastern Australia, including the Murray Darling Basin and coastal NSW [125]. The source of atmospheric rivers influencing coastal and inland NSW are the western Pacific and southern Indian Ocean, which are more likely to develop in La Niña conditions [125].

3.3.3.1 Datasets

No publicly available datasets are listed in the publications. The Australian datasets may be available through contacting the authors of Reid et al. [125]

3.3.4 Anticyclones (high pressure systems)

The mid-latitude eastward propagation of extratropical cyclone systems are frequently interrupted by prolonged periods of atmospheric blocking, which are quasi stationary high-pressure systems that occur at higher latitudes than the subtropical high pressure belt [132]. In the Southern Hemisphere, the formation of blocking high-pressure systems is influenced by the configuration of atmospheric long waves, or Rossby waves,

and are predominantly observed at a mean latitude of 45°S to the east ('downstream' in an atmospheric sense) of the continents in the western Pacific, western Atlantic and western Indian Ocean [132,133].

The blocking high-pressure systems deflects the eastward travelling cyclones over the Southern Ocean to the south and north, leading to a significant redistribution of heat and moisture around the high-pressure system [132]. Blocking in the Tasman Sea influences precipitation over southeast Australia, New Zealand and East Antarctica, with some regions receiving persistent and/or extreme precipitation (e.g., subtropical eastern Australia, East Antarctic coastline) while other regions are dry (e.g., western Tasmania, New Zealand)[5,134,135]. Over Australia, the influence of atmospheric blocking on rainfall variability and extremes depends on the precise location of the block and interaction with other weather types (i.e., troughs, low-pressure systems)[5,9]. Atmospheric blocking in the Tasman Sea region favours increased rainfall over the NSW coast, through enhanced easterly winds [3,5,82]. Atmospheric blocking in the Tasman Sea can also be associated with the development of cut-off lows (related to east coast lows), to the west of the high-pressure system which leads to heavy widespread rainfall over both inland and coastal NSW [122,136]. A cut off low forms when a pool of cold upper air breaks away from the main subpolar circulation, often initiated by a blocking high-pressure system to the east. These systems are associated with moderate to heavy rainfall across southeast Australia (up to 70% of heavy rainfall events can be attributed to cut off lows), and as such are particularly important for agriculture and urban water security [4,122,136–138]. The frequency and intensity of these systems are influenced by the phase of SAM (increased frequency in SAM+) and sea surface temperature anomalies to the south and north of Australia [4,5,82].

3.3.4.1 Datasets

The weather typing datasets used in in Pepler et al.[7,123] are an output of the Victorian Water and Climate Initiative and available for research purposes by contacting the authors.

Tasman Sea high pressure systems are also represented by SOM6, SOM7 and SOM8 in Udy et al. [82]. The daily synoptic typing dataset from January 1979 to October 2018 can be downloaded from the Australian Antarctic Data Centre: https://data.aad.gov.au/metadata/AAS_4537_z500_SynopticTyping_SouthernIndianOcean

4 Dominant drivers for NSW rainfall

Multiple studies have compared the individual influence of either modes of climate variability or synoptic weather conditions on eastern Australian rainfall. Additionally, there has been substantial research into the combined influence and interactions between IOD and ENSO on southeast Australia rainfall [5,73,139,140]. However, there are limited studies that compare the influence and interaction of more than two modes of variability and/or weather systems on NSW rainfall. Additionally, the time-period, indicies and methods used across the studies vary which results in different results due to the time-period sensitivity of correlation scores between a driver and rainfall data. For example, different regions of NSW have significant correlation results for ENSO, SAM and/or IOD between Risbey et al.[5], Black and Lane[1] and McKay et al[141]. This makes it difficult to distinguish a dominant driver of rainfall at regional scales.

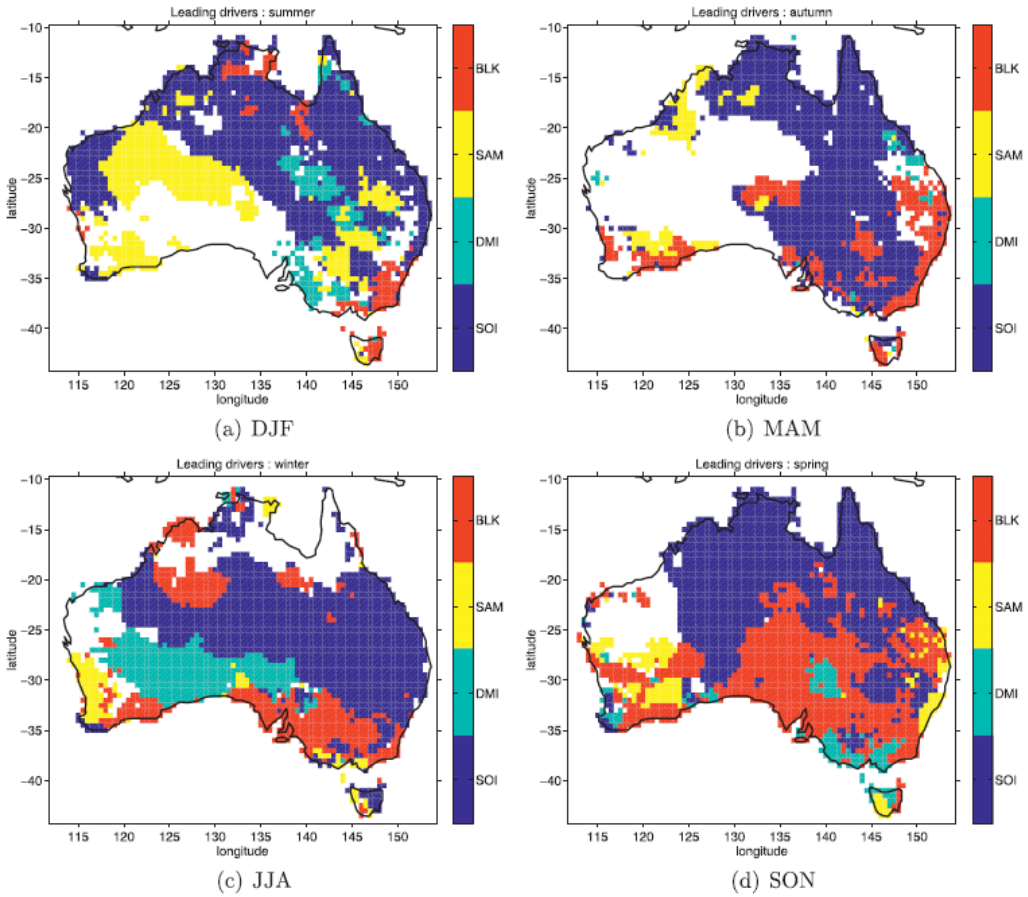

Figure 18: Dominant climate driver at grid point (out of blocking (blk in figure), Southern Annular Mode (SAM in figure), Indian Ocean Dipole (DMI in figure) and El Niño Southern Oscillation (SOI in figure) for each season. Strongest correlation score between monthly rainfall and climate driver index used to determine the dominant driver. Source: Risbey et al.[5]

Two studies that compare more than two modes of variability and/or weather systems on southern Australia rainfall are Risbey et al.[5] and McKay et al. [141]. Risbey et al.[5] compared the influence of three modes of climate variability (ENSO, SAM, IOD) and atmospheric blocking. They identified the 'dominant' driver of rainfall variability based on the strongest correlation score. During winter, ENSO is the dominant driver of rainfall variability across most of NSW, except for blocking in parts of southern NSW (Figure 18).

Spring, summer and autumn rainfall have multiple drivers across NSW. Spring rainfall over coastal NSW has the strongest relationship with SAM in the northern and central regions and blocking in the south. Northern inland NSW is influenced by a mix between blocking, SAM and ENSO, while rainfall variability across the southern inland regions has the strongest relationship with blocking. Summer rainfall along coastal NSW has the strongest relationship with ENSO in the northern and central regions and blocking in the south. Inland NSW is influenced by a mix between SAM, ENSO or no dominant driver identified (out of the four in the study). Autumn rainfall is

split by blocking over coastal NSW and predominately ENSO over inland NSW [5]. It is important to note the rainfall data used in Risbey et al.[5] only extended to 2006, missing the past 15+ years of data which includes an IPO negative period, record ENSO, SAM and IOD events and extreme wet and dry conditions.

McKay et al.[141] reviewed existing literature on the long-term changes in synoptic to large-scale atmospheric circulation and impact on rainfall across Southern Australia. This study included updated correlation maps for relationships between climate modes (Central Pacific ENSO, Eastern Pacific ENSO, IOD and SAM) and Australian rainfall between 1979-2019. The NSW regions with significant correlations between modes of climate variability and seasonal rainfall in McKay et al.[141] differ from correlation maps in Risbey et al.[5], likely due to different time periods and datasets used in each study. The key differences are related to the influence of ENSO and SAM on summer rainfall across NSW. McKay et al[141] found that neither central or eastern Pacific ENSO events have any significant influence on summer rainfall, while SAM has a significant influence along the entire NSW coast and parts of inland NSW.

The influential synoptic-scale weather systems and main climate drivers for coastal and inland NSW during late autumn to early spring (~May to October) and late spring to early autumn (November to March) is summarised in Table 2.

Table 2: Summary of regional rainfall seasonality, mechanisms required for rainfall and the influence of climate modes of variability and weather systems on NSW rainfall variability. Weather and climate drivers with limited influence are grey.

Regions	Dominate rainfall season	Mechanism(s) required for rainfall	Rainfall drivers - May to October	Rainfall drivers – November to April
Coastal (north /central) Far North Coast, North coast, Greater Hunter and Greater Sydney	Summer dominated with low winter rainfall.	The proximity to warm Pacific Ocean means that surface onshore easterly winds increase moisture input into the region. This leads to rainfall when the moist air parcel is uplifted over the Great Dividing Range. Weather systems can also enhance the vertical uplift which can increase rainfall intensity and spatial coverage of rainfall event. The ECFI and GDI indices both the easterly wind component and ECFI also captures the vertical motion.	**IPO:** Negative phase linked to stronger relationship between ENSO and IOD to southeast Australia rainfall. Also linked to weaker ENSO-IOD co-variability and promotes SAM+ conditions. **ENSO**: Weak / limited influence over coastal NSW **IOD**: not significantly related to rainfall variability over coastal NSW, but the phase can override any ENSO signal - IOD+ enhances surface easterly wind strength -> increased chance of winter rainfall. **SAM**: Limited / no influence over coastal NSW **MJO**: Phase 4 and 5 increased rainfall along NSW coast in autumn and winter **East coast cyclones**: ECLs contribute 15-25% of May-October rainfall between 1970 - 2006 [142]. ECL related rainfall more likely in SAM+ conditions. **Cold fronts**: reduced rainfall across coastal NSW (descending air -> inhibiting convection and rainfall). **Atmospheric rivers**: ARs contribute 30-40% of winter rainfall along the NSW coast. **Tasman Sea high pressure systems:** Blocking at 140°E associated with increased rainfall along the NSW coast	**IPO:** Negative phase linked to stronger relationship between ENSO and IOD to southeast Australia rainfall. Also linked to weaker ENSO-IOD co-variability and promotes SAM+ conditions. **ENSO:** La Niña enhances surface easterly wind strength -> increased chance of rainfall. El Niño reduces surface easterly winds -> rainfall suppressed over coastal NSW. [5,143] **IOD:** Limited influence. IOD events decay in late spring / early summer with the arrival of the Australian monsoon. **SAM:** Positive phase enhances easterly surface wind and vertical motion -> increased chance of widespread rainfall. Negative phase reduces surface easterly winds / shifts to westerly winds -> rainfall suppressed over coastal NSW (Hendon et al, 2007). **MJO:** No significant correlations **East coast cyclones:** ECLs contribute 10-20% of November-April rainfall between 1970 – 2006 [142]. ECL related rainfall more likely in SAM+ conditions. **Cold fronts:** reduced rainfall across coastal NSW (descending air -> inhibiting convection and rainfall). **Atmospheric rivers:** ARs contribute up to 30% of summer rainfall over northern NSW coast. Source region predominately western Pacific. **Tasman Sea high pressure systems:** Blocking at 140°E associated with increased rainfall over south coast.

Regions	Dominate rainfall season	Mechanism(s) required for rainfall	Rainfall drivers - May to October	Rainfall drivers – November to April
South coast	Uniform	Surface easterly flow Summer: easterly winds dominate Winter: equal split between easterly and westerly wind anomalies but 60% of rainfall associated with easterly wind days. Westerly wind days lead to subsidence and inhibit rainfall over coastal NSW	IPO: Negative phase linked to stronger relationship between ENSO and IOD to southeast Australia rainfall. Also linked to weaker ENSO-IOD co-variability and promotes SAM+ conditions. ENSO: Weak / limited influence over coastal NSW IOD: not significantly related to rainfall variability over coastal NSW, but the phase can override any ENSO signal - IOD+ enhances surface easterly wind strength -> increased chance of winter rainfall. SAM: Limited / no influence over southern coastal NSW in JJA. Positive SAM increased chance of rainfall in SON. MJO: Phase 4 and 5 increased rainfall along NSW coast in autumn and winter. Phase 6 increased rainfall in spring over NSW south coast. East coast cyclones: ECLs responsible for 30-50% of May to October rainfall (1970 – 2006) [142] Cold fronts: associated with westerly wind regime which results in subsidence and dry conditions along the coast. Atmospheric rivers: ARs contribute 30-40% of winter rainfall along the NSW coast. Tasman Sea high pressure systems: Blocking at 140°E associated with increased rainfall over southern NSW coast in autumn, winter and spring.	IPO: Negative phase linked to stronger relationship between ENSO and IOD to southeast Australia rainfall. Also linked to weaker ENSO-IOD co-variability and promotes SAM+ conditions. ENSO: La Niña enhances surface easterly wind strength -> increased chance of rainfall. El Niño reduces surface easterly winds / shifts to westerly winds -> rainfall suppressed over coastal NSW. IOD: Limited influence. IOD events decay in late spring / early summer with the arrival of the Australian monsoon. SAM: Positive phase enhances easterly surface wind and vertical motion -> increased chance of widespread rainfall. Negative phase reduces surface easterly winds / shifts to westerly winds -> rainfall suppressed over coastal NSW MJO: No significant correlations East coast cyclones: ECLs responsible for up to 20% of November to April rainfall (1970 – 2006) Cold fronts: associated with westerly wind regime which results in subsidence and dry conditions along the coast. Atmospheric rivers: ARs contribute up to 20% of summer rainfall over southern NSW coast. Tasman Sea high pressure systems: Blocking at 140°E associated with increased rainfall over southern NSW coast in summer.

Regions	Dominate rainfall season	Mechanism(s) required for rainfall	Rainfall drivers - May to October	Rainfall drivers – November to April
Inland: Northern / Central Border Rivers, Gwydir, Namoi, Macquarie-Castlereagh, Lachlan	Summer / uniform	Easterly surface flow and vertical motion in atmosphere (i.e. convection)	**IPO:** Negative phase linked to stronger relationship between ENSO and IOD to southeast Australia rainfall. Also linked to weaker ENSO-IOD co-variability and promotes SAM+ conditions. **ENSO**: La Niña -> increased chance of rainfall. El Niño -> reduced chance of rainfall. **IOD**: Negative -> increased chance of rainfall. Positive -> decreased chance of rainfall. **SAM**: JJA - limited influence. SON – positive (negative) phase increases (decreases) chance of rainfall. **MJO**: Phase 5 associated with anomalous low pressure over southeast Australia -> increased rainfall chance (odds ratio = 1.2) in parts of north/central inland NSW. Phase 3 associated with anomalous high pressure over southeast Australia -> decreased rainfall chance over parts of central inland NSW (odds ratio = 0.7) **East coast cyclones**: Continental lows (e.g. cut off lows represented by cluster 4/5) are associated with increased rainfall over northern/central inland NSW. More likely in SAM+ in winter **Cold fronts**: <10% of autumn, winter and spring rainfall **Atmospheric rivers**: ARs contribute 30-40% of autumn, winter and spring rainfall over inland NSW [125]. **Tasman Sea high pressure systems:** Blocking at 140°E associated with increased rainfall over inland NSW coast in autumn, winter and spring. Rainfall result of an extra-tropical cyclone stalled over inland NSW due to blocking high in Tasman.	**IPO:** Negative phase linked to stronger relationship between ENSO and IOD to southeast Australia rainfall. Also linked to weaker ENSO-IOD co-variability and promotes SAM+ conditions. **ENSO**: La Niña enhances surface easterly wind strength -> increased chance of rainfall. El Niño reduces surface easterly winds / shifts to westerly winds -> reduces chance of rainfall **IOD**: Limited influence. IOD events decay in late spring / early summer with the arrival of the Australian monsoon. **SAM**: parts of inland NSW have significant relationship to SAM in DJF – focussed northeast inland NSW. **MJO**: Phase 4 increases summer rainfall by 1.3x over northwest NSW. Other regions no influence **East coast cyclones**: Continental lows (e.g. cut off lows represented by cluster 4/5) are associated with increased rainfall over northern / central inland NSW. More likely in SAM+ in summer **Cold fronts**: 2.5-5% of summer rainfall **Atmospheric rivers**: ARs contribute up to 30% of summer rainfall over northeast inland NSW (e.g. northern MDB). **Tasman Sea high pressure systems:** No significant correlations with blocking at 140°E over summer

Regions	Dominate rainfall season	Mechanism(s) required for rainfall	Rainfall drivers - May to October	Rainfall drivers – November to April
Southern inland: Murrumbidgee, Murray	Winter	Westerly flow (e.g. cold front) in winter increases rainfall through orographic uplift on western side of Great Dividing Range. Westerly flow in summer associated with dry conditions due to shift in subtropical jet and warm/dry inland Australia. Summer rainfall also associated with thunderstorms and tropical systems	**IPO:** Negative phase linked to stronger relationship between ENSO and IOD to southeast Australia rainfall. Also linked to weaker ENSO-IOD co-variability and promotes SAM+ conditions. **ENSO**: La Niña -> increased chance of rainfall. El Niño -> reduced chance of rainfall. **IOD**: Negative -> increased chance of rainfall. Positive -> decreased chance of rainfall. **SAM**: NSW/Vic border region: negative (positive) SAM increases (decreases) chance of rainfall through increased (decreased) frequency of cold fronts **MJO**: Phase 5 associated with anomalous low pressure over southeast Australia -> increased rainfall chance. Phase 3 associated with anomalous high pressure over southeast Australia -> decreased rainfall chance. **East coast cyclones**: Continental lows (e.g. cut off lows represented by cluster 4/5) are associated with increased rainfall over southern inland NSW. More likely in SAM+ **Cold fronts**: 15-25% of autumn, winter and spring rainfall. More likely in SAM- in JJA. **Atmospheric rivers**: ARs contribute 30-40% of autumn, winter and spring rainfall over inland NSW. Source region is predominately the Southern Ocean and associated with a cold front. **Tasman Sea high pressure systems:** Blocking at 140°E associated with increased rainfall over inland NSW coast in autumn, winter and spring	**IPO:** Negative phase linked to stronger relationship between ENSO and IOD to southeast Australia rainfall. Also linked to weaker ENSO-IOD co-variability and promotes SAM+ conditions. **ENSO**: La Niña enhances surface easterly wind strength -> increased chance of rainfall. El Niño reduces surface easterly winds / shifts to westerly winds -> reduces chance of rainfall. **IOD**: Limited influence. IOD events decay in late spring / early summer with the arrival of the Australian monsoon. **SAM**: Positive (negative) SAM increases (decreases) rainfall **MJO**: no significant relationships with rainfall variability **East coast cyclones**: Continental lows (e.g. cut off lows represented by cluster 4/5) are associated with increased rainfall over southern inland NSW. More likely in SAM+ **Cold fronts**: less than 2.5% of summer rainfall (front alone). If combined with cyclone and thunderstorms contribute up to 30% of summer rainfall (*note region is drier in summer*). **Atmospheric rivers**: ARs contribute 10-20% of summer rainfall over southern inland NSW. **Tasman Sea high pressure systems:** Blocking at 140°E increases chance of rainfall over southern inland NSW west of the Great Dividing Range. No influence further west.

5 Simulation of weather and climate drivers in climate models

This section summarises model evaluation studies related to modes of climate variability (Section 5.1) and synoptic weather systems (Section 5.2) important for rainfall across NSW and their projected changes. Model biases are also considered for how they may influence the rainfall teleconnection across NSW. The number of relevant model evaluation studies varies from single papers for some modes of variability / weather systems (i.e. atmospheric rivers) to extensively studied (i.e. ENSO).

This review includes evaluation studies based on climate models that have participated in the 3rd, 5th and/or 6th Coupled Model Intercomparison Projects (CMIP) and regional climate models (RCMs) over the Australian domain. The RCMs include outputs from the New South Wales and Australian Capital Territory Regional Climate Model (NARCliM), Conformal Cubic Atmospheric Model (CCAM) and the Bureau of Meteorology Atmospheric Regional Projections for Australia (BARPA).

5.1 Simulation of modes of climate variability and their projected changes

Climate models credibly represent the spatial patterns of the key climate variability modes that influence NSW rainfall. However, the dynamics of the climate variability modes are poorly represented resulting in underestimation or overestimation of the amplitude and temporal variability (i.e. length of phases). Poor dynamic representation also causes biases in the rainfall teleconnection to NSW which influences regional rainfall projections.

The frequency of extreme ENSO and IOD events are projected to increase, likely causing frequent fluctuations between drought and flood conditions in NSW. The continued shift to positive SAM in summer up until ~2050 is projected to be weaker than the observed shift to positive SAM between 1980 to 2000 due to opposing influence of stratospheric ozone hole recovery and increased greenhouse gases. Post 2050, SAM is projected to shift to the positive state in all seasons under high emission scenarios. The impact of positive SAM shift on NSW rainfall depends on the season and region. During winter less rainfall is likely over southern inland NSW due to reduction in frequency of extra-tropical cyclones and cold fronts. During summer increased rainfall is likely over coastal and northern inland parts of NSW due to strengthened easterly winds.

IPO predictions are less clear, with no clear model consensus for amplitude or phase shifts up until 2050. Post 2050 there is *medium confidence* that Pacific decadal variability may become weaker but the phase changes may happen with higher frequency.

5.1.1 IPO

There are limited model evaluation studies related specifically to IPO simulation, however more studies are available on the northern Pacific component of decadal variability in the Pacific Ocean – the Pacific Decadal Oscillation (PDO).

5.1.1.1 Evaluation

CMIP5 pre-industrial and forced historical runs generally underestimate IPO decadal scale variability. The majority of models are biased towards simulating more IPO events per century with reduced duration compared to observations [144]. Observations range between 6-7 IPO events per century with a mean phase length of 14-18 years. In contrast, the control and historical forcing model simulations generate between 8-9 IPO events per century with mean phase lengths between 10-12 years (Figure 19).

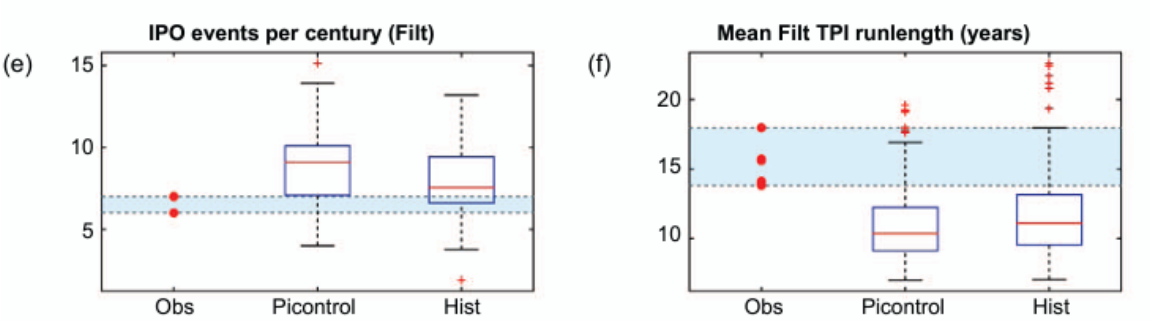

Figure 18: Observed and modelled IPO metrics. Left – number of IPO events per century. Right – mean event length. Boxplot boundaries represent the 25th and 75th percentiles, red line the median value and whiskers show the extend of data not considered outliers. Outliers are shown as red dots. Source: Henley et al.[144]

Figure 20 shows that the spatial representation of IPO SST variability is credible with spatial pattern correlation scores between each model and observations ranging between 0.4 and 0.8 (note a score of 1 is perfect match). SST biases across the tropical region are less than +/- 0.2°C for both positive and negative phases, while the extratropical regions have biases up to +/- 0.4°C [144]. The larger SST bias in the extratropical region is consistent with PDO evaluation studies [145,146]. The magnitude of this SST bias has decreased (i.e. the model has improved) over the successive CMIP generations which has improved spatial pattern correlation scores relative to observations [145].

Models that realistically represent the spatial representation of IPO and have lower temporal biases in the number of IPO events/run length include ACCESS1-0, ACCESS1-3, CMCC-CM, CSIRO-Mk3-6-0, MPI-ESM-LR, MPI-ESM-MR, MPI-ESM-P, MRI-CGCM3 and NorESM1-M [144]. However, it is important to note that it is still uncertain whether the dynamics and feedbacks related to IPO variability are correctly captured in these models as the physical mechanisms for multi-decadal variability (e.g. internally or externally forced) are still unknown and remains an active area of research[41]. Additionally, the models that capture IPO spatial representation credibly do not align with the models that perform best for ENSO variability and NSW rainfall teleconnection [147,148].

The temporal biases in IPO simulation may influence NSW rainfall predictions due to the inability to simulate multi-decadal dry or wet phases that have occurred in the observation and palaeoclimate records [19,23,36,42]. The spatial biases also likely influence the teleconnection to NSW rainfall through related changes in the walker circulation and intertropical convergence zones [149,150].

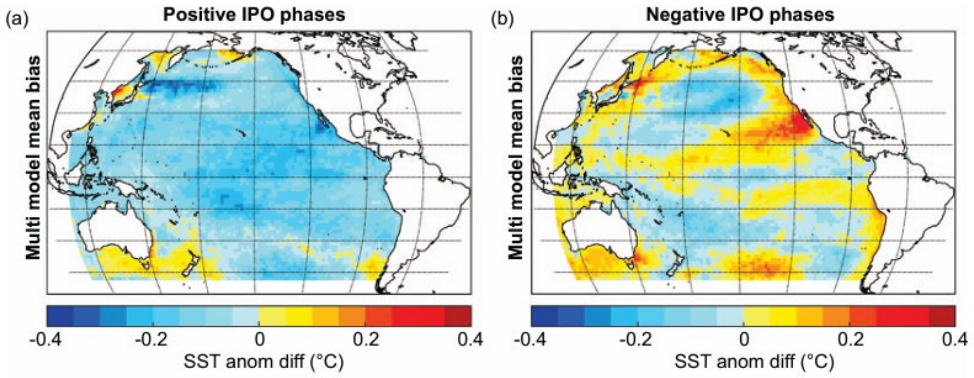

Figure 19: IPO spatial SST model bias for positive and negative phases. Specifically, a region with a positive temperature bias means the model is overestimating sea surface temperatures, while a region with a negative temperature bias is underestimating sea surface temperature indicating potential errors in the model dynamic and feedback mechanisms related to IPO. Source: Henley et al.[144]

5.1.1.2 Projection

The near-term (to 2050) predictions are highly dependent on model selection, with no clear model consensus for amplitude or phase shifts. Pacific decadal variability can also mask or amplify climate change trends which is

likely to continue in the near-term [151]. Over mid-long term periods (post 2050) there is medium confidence based on CMIP5 models that Pacific decadal variability may become weaker but phase changes could happen with higher frequency [151].

5.1.2 ENSO

ENSO simulation and projection in CMIP models has been extensively studied, with significant improvements in model bias over the successive CMIP generations. However, uncertainties still exist for how well the latest CMIP6 models capture the fundamental dynamics of ENSO and there is limited consensus in the literature on the future amplitude of ENSO variability.

5.1.2.1 Evaluation

ENSO spatial variability is simulated relatively well in both CMIP5 and CMIP6 models, however the ENSO dynamics and feedbacks (e.g. wind stress, thermocline tilt) are poorly simulated which limits confidence in ENSO amplitude and phase projections [152]. The poor dynamic representation of ENSO also influences the climate teleconnections associated with ENSO variability [152,153]. The majority of CMIP5 and CMIP6 models display biases in the mean climate state compared to observations, with cold biases in the western Pacific and warm biases in the eastern Pacific (Figure 21) [154]. For example, 81% of CMIP5 and 93% of CMIP6 models have a cold equatorial bias in the western Pacific basin which contributes to a more 'La Niña' like state response to increasing greenhouse gases [148,154]. The cold equatorial SST bias also influences rainfall projections is regions have teleconnections to ENSO variability [148]. Models with more 'realistic' ENSO dynamics and feedbacks generally have reduced equatorial cold SST bias and non-linear ENSO behaviour [152]. These CMIP6 models include CAMS-CSM1.0, CESM2-WACCM, FGOALS-F3-L, MIROC6, MRI-ESM2.0, NorESM2-MM.

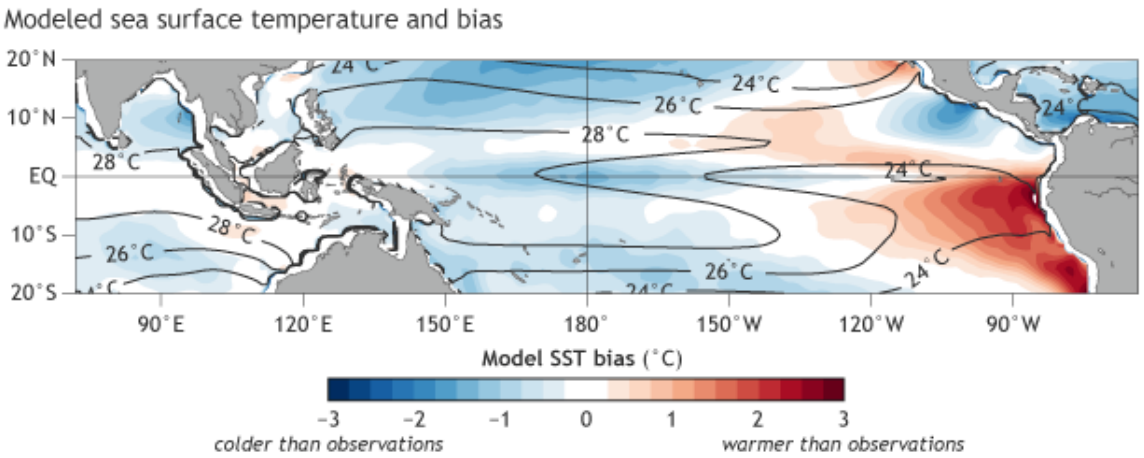

Figure 20: CMIP5 multi-model ensemble mean sea surface temperature bias compared to observations. The cold equatorial SST bias extends further west in models compared to observations. Source: NOAA *https://www.climate.gov/news-features/blogs/enso/challenges-enso-today's-climate-models*

For eastern Australia, only a limited number of CMIP5 and CMIP6 models simulate both historical ENSO variability and the ENSO rainfall teleconnection [147,148] (Figure 22). CMIP6 models have improved their ability to represent ENSO variability (including reduced cold SST biases) but only a subset (e.g. CanESM5, GFDL-ESM4 and MRI-ESM2-0) also simulate the observed teleconnection to eastern Australian rainfall. [147]. Additionally, models that perform well for other aspects of Australian climate (e.g. temperature and precipitation) perform less favourably with respect to ENSO (e.g. CNRM-CM6-1-HR, GISS-E2-1-G, HadGEM3-GC31-LL, and UKESM1-0-LL [147].

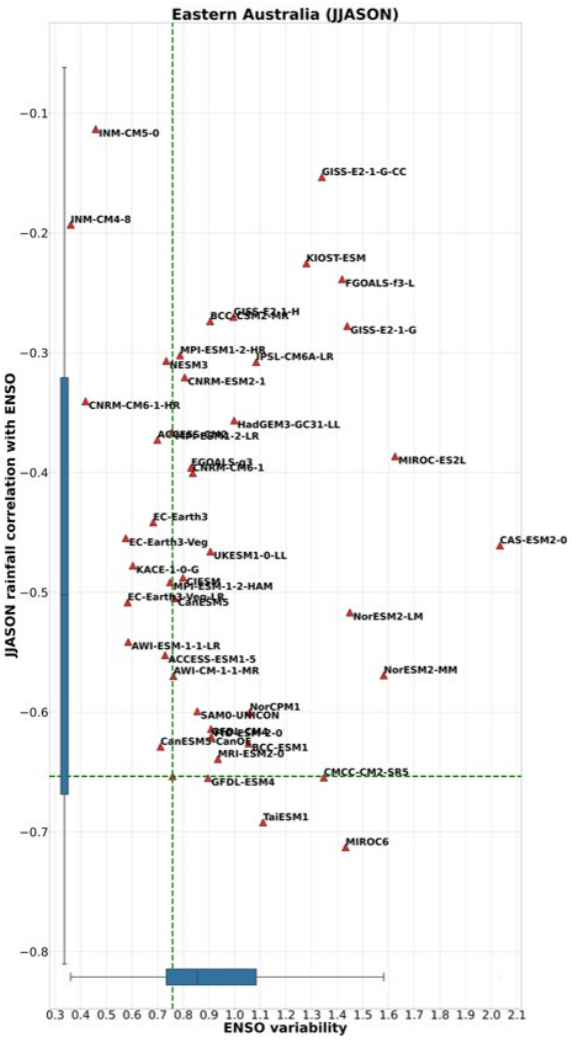

Figure 21: Spread of CMIP6 models' ability to simulate ENSO variability and rainfall teleconnection to eastern Australia NRM region (July to November). Each model evaluated is represented by a red triangle. The green dashed line represents observed conditions over 1950 – 2014. Models that are performing well at simulating both ENSO variability and NSW rainfall teleconnections should be close to these green dashed lines. Source: Di Virgilio et al.[147]

5.1.2.2 Projection

The AR6 Climate Change 2021 Physical Science basis reports that 'it is *virtually certain* that ENSO will remain the dominant mode of interannual variability in a warmer world'. However, there is currently no model consensus for a systematic change in the intensity of ENSO SST variability over the 21st century in any of the emission scenarios assessed (*medium confidence*). The IPCC 2021 report also states that is *very likely* that ENSO rainfall variability within the Niño3.4 region will increase significantly regardless of amplitude changes in ENSO SST variability by the second half of the century in SSP2-4.5, SSP3-7 and SSP5-8.5 [151]. However studies published after the cut-off date for AR6 synthesis disagree with the latest IPCC conclusions (partially due increased number of models available), finding that ENSO SST variability and extreme events are projected to increase with a stronger inter-model consensus in CMIP6 compared to CMIP5 [155–157].

The ENSO teleconnection to eastern Australian rainfall is projected to stay relatively consistent with historical teleconnection observations [153].

5.1.3 IOD

Evaluation and projections of IOD in CMIP5 and CMIP6 have been moderately studied.

5.1.3.1 Evaluation

The spatial pattern of IOD is reasonably well represented in CMIP3, CMIP5 and CMIP6 models, however the amplitude of the SST anomalies is larger than observations [147,158,159]. The amplitude of IOD is also asymmetric in observations (i.e. positive events are much stronger than negative), which is poorly represented in CMIP5 and CMIP6 models [160]. CMIP5 and CMIP6 models also display a climate mean bias across the equatorial region of the Indian Ocean which unrealistically tilts the west to east thermocline towards the eastern Indian Ocean, leading to a positive IOD SST pattern as the mean climate state [159,161]. The seasonality of the peak of IOD shifted from November in CMIP5 to September in CMIP6, compared to observational peak between August and October [161].

The observed teleconnection between tropical Indian Ocean SST variability and precipitation across south-eastern Australia is captured in CMIP5 and CMIP6 models [147,159,160]. However, the observed rainfall teleconnection is also sensitive to the IOD amplitude which is too large in CMIP5 and CMIP6 models [159]. This overestimation of IOD amplitude in the model simulations likely overestimates rainfall decline projections in regions influenced by IOD variability (e.g. southern NSW during winter/spring).

Additionally, the CMIP5 and CMIP6 models that best represent IOD variability and the rainfall teleconnection to southeast Australia well are often not consistent with the models that best represent ENSO variability and the rainfall teleconnection to eastern Australia [147]. CMIP5 models also display a weak IOD to ENSO relationship compared to observations [159]. This makes it difficult to assess the compound influence that the two modes of variability have when acting together in the future due to limited models (e.g. increased chance of above average rainfall conditions when La Niña and negative IOD co-occur / increase chance of below average rainfall conditions when El Niño and positive IOD co-occur).

5.1.3.2 Projection

CMIP5 and CMIP6 models that reasonably represent IOD events project that further increases in greenhouse gas emissions during the 21st century could accelerate the warming of the western Indian Ocean and tilt the thermocline to the east which would shift the future mean climate state of the Indian Ocean to a positive IOD pattern [158,160,162,163]. This shift in the mean climate state would make the development of extreme positive IOD events more likely [158,163]. If warming is limited to the 1.5°C Paris agreement the frequency of extreme positive IOD events is projected to stabilise at double the frequency of pre-industrial periods, while continuing warming during the 21st century could result in a tripling of extreme positive IOD event frequency [162] Even with this limited warming, a projected doubling of IOD positive events will likely increase drought and fire hazard across southern NSW [93].

5.1.4 SAM

The trends, spatial structure and amplitude of SAM variability in CMIP models have been moderately studied.

5.1.4.1 Evaluation

The spatial pattern of SAM in all seasons is realistically captured in CMIP6 model, with spatial pattern correlation scores greater than 0.8 for the 16 models evaluated [164]. Both CMIP5 and CMIP6 models show an improvement compared to CMIP3 in simulating the spatial pattern of SAM [145,164,165]. The highest pattern correlations in the CMIP6 models are observed in summer (correlation scores >0.95) and weakest in autumn (correlation scores range between 0.8 – 0.9) [164].

SAM amplitude is poorly represented in CMIP5 and CMIP6 models, with models either overestimating (including MIROC-ESM-CHEM, FGOALS-s2, and BCC_CSM1.1) or underestimating the strength of the pattern [164]. The amplitude bias may be partially due to the asymmetric component of the SAM [79,81] not accurately simulated in CMIP models [164]. At an annual scale the zonal average of north to south pressure difference characterised as the symmetric component of SAM can be realistically represented by the CMIP models [164]. However, the higher frequency asymmetric component of SAM (i.e. synoptic-weather scale features) which is important for rainfall extremes in southeast Australia are less accurately represented in CMIP models [164]. This potentially has implications for the SAM rainfall teleconnections to NSW and rainfall projections in regions that are sensitive to the asymmetric component of SAM, particularly coastal NSW and northern Murray Darling Basin regions (i.e. lack of asymmetric structure in summer reduces summer rainfall) [3,83].

Realistically simulating SAM amplitude and trends also appears to be influenced by the representation of stratospheric ozone in the model. In models with interactive ozone chemistry, the observed strengthening of SAM in summer is attributed nearly completely to ozone depletion with minimal influence from greenhouse gases due to feedback mechanisms between stratospheric ozone and greenhouse gases [166]. However, in models with prescribed ozone (i.e. static concentrations) the strengthening of SAM is attributed to both ozone depletion and greenhouse gas increases [84]. Most CMIP6 models do not have interactive ozone chemistry which results in biases in southern hemisphere climate trends [167] and may impact future projections and rainfall teleconnections related to SAM variability. To reduce the biases, the CMIP6 modelling protocol for models without interactive chemistry recommended the use of prescribed 4-dimensional monthly mean ozone concentration rather than previously used zonal mean values or linear interpolation [167–169].

5.1.4.2 Projection

The AR6 Climate Change 2021 Physical Science basis concluded with *high confidence* that in the near term the greenhouse gas forced change in SAM in austral summer to the positive phase is likely to be weaker than observed during the late 20th century under all 5 SSPs due to the opposing influence of stratospheric ozone hole recovery (return to neutral conditions) and increases in greenhouse gases (forcing SAM+ in all seasons). In addition, the forced changes in SAM in the near term are likely to be smaller than natural variability changes. In the long-term SAM is likely to shift to a positive state across all seasons, representing a poleward shift in the mid-latitude jet and increased wind speeds associated with extratropical cyclones, under high emission scenario (SSP5-8.5) relative to 1995-2014. Low emission scenarios (SSP1-2.6) in CMIP6 models do not project any robust change in the SAM index in the long term [151].

A shift to positive SAM in all seasons will have varying seasonal influences on rainfall across NSW. During winter, less rainfall is likely in the southern regions due to a reduction in frequency of cyclones and cold fronts associated with positive SAM conditions [89]. However, during summer the circulation anomalies associated with positive SAM increase the chance of rainfall over coastal regions by directing warm moist air onshore [89].

5.1.5 MJO

5.1.5.1 Evaluation

CMIP6 models simulate the MJO eastward propagation more realistically than CMIP5 models but still underestimate the magnitude and frequency of initiation events over the Indian Ocean [170–173]. The tropical precipitation variability associated with MJO in CMIP6 models is also underestimated over northern Australia and the extra-tropical rainfall teleconnections are poorly represented [172].

5.1.5.2 Projection

CMIP6 models that have realistic MJO eastward propagation in their historical runs project a decrease in MJO precipitation amplitude (10-20%) and increased propagation speed (~9%) [174].

5.2 Simulation of synoptic-scale weather systems and their projected changes

The spatial scale of weather systems important for NSW rainfall influences the ability for climate models to simulate them. CMIP models are broadly able to capture the shape and structure of large extra-tropical cyclones and anticyclones. However, the frequency is underestimated for cyclones and overestimated for anticyclones which impacts NSW rainfall projections. Smaller cyclones, including east coast lows, are poorly simulated in CMIP models due to large spatial grid resolution of CMIP models (~200km) and short timescale of east coast lows (2-3 days). Dynamically downscaled regional climate models improve the representation, frequency and associated rainfall processes of cyclones and anticyclones in the NSW region.

The frequency of east coast lows, extra-tropical cyclones and associated frontal systems are projected to decline in the cool season. However, summer frequency and intense cyclones with heavier rainfall over the NSW coast are projected to increase. This reflects a shift in distribution, with less cyclone days overall but more intense cyclones with increased rainfall rate. Its important to consider the projected distribution shift in the context of historical and palaeoclimate evidence of extreme events.

5.2.1 Cyclones and cold fronts (including east coast cyclones and extra-tropical cyclones)

Australian specific model evaluation studies related to east coast cyclones, extra-tropical cyclones, cold fronts and their influence on rainfall projections is an active area of research. There is a decent amount of literature (~5 studies in the past decade) on the evaluation and/or projections of east coast low and extra-tropical over the Australian domain, often with a focus on the east coast [175–179]. However, there are limited studies that directly assess the ability of CMIP6 models to simulate cold fronts and associated rainfall in the Australian domain. The evaluation and projections of frontal systems can be inferred from analysis of extra-tropical cyclones, and associated frontal systems [e.g. 178], global storm track studies [e.g. 180,181] or case studies of extreme frontal events [e.g. 182,183].

5.2.1.1 Evaluation

Over southern Australia, CMIP5 models simulate larger extra-tropical cyclones but underestimate the frequency of both surface and upper level (500hPa) cyclones, producing around 60% as many surface lows and 30% of upper-level lows compared to reanalysis observational datasets (e.g. ERA5, JRA-55 and BARRA) [178]. Smaller spatial scale cyclones, such as east coast lows / east coast cyclones, are poorly simulated and challenging to model due to the spatial scale difference between the global circulation model grid size (~200km) and the relatively small spatial scale of east coast lows, the short timescale between cyclone development and decay (2-3 days) and multiple origins (e.g. near the coast of NSW, over inland regions or the tropics) [176].

However, dynamical downscaling to finer spatial resolution with regional climate models (RCM) (e.g. NARCliM project for NSW) has improved the representation of cyclones and their associated rainfall processes particularly along the coasts and over elevated topography [176,184]. The NARCliM1.0 [185] RCM ensemble mean is able to effectively simulate mean cyclone duration, mean cyclone size, mean sea level pressure gradient and number of events per year to within observational uncertainty [176]. However, the spread of individual models is larger than observational uncertainty and no subset of models stand out as individually well performing across all evaluation metrics or seasons (warm/cold) [176].

A different subset of RCMs (mix of NARCliM1.5 [186], CCAM and BARPA) also shows improvement in cyclone frequency, structure and precipitation impacts compared to the CMIP5 models [178]. In the RCMs, the model bias (compared to ERA5 reanalysis observations) for the average number of surface and upper cyclones is reduced by 5-10% across NSW. The characteristics of eastern seaboard cyclones, including rain rate, instantaneous wind speed and mean sea level pressure are effectively simulated at both the surface and upper levels (Figure 23) [178]. While the model mean displays relatively low biases in cyclone characteristics, individual models have larger biases particularly related to shallow cyclones in southeast Australia [178]. The spatial pattern of contribution of surface and upper level cyclones to annual rainfall is relatively consistent across NSW between ERA5 and the RCM ensemble mean, however the models generally underestimate the contribution by 5-10% [178].

Case study evaluations of intense cold fronts indicates the coarse spatial resolution of CMIP models underestimates the temperature gradient and curvature of frontal systems which likely influences the amount of rainfall associated with cold fronts. The representation of cold fronts is improved in downscaled models [182].

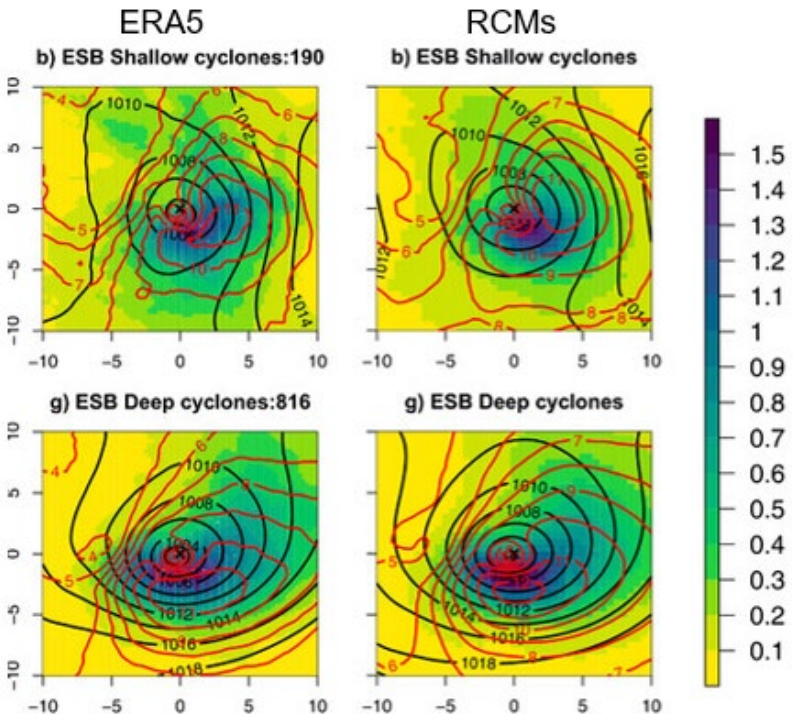

Figure 22: Composite mean rain rate (shaded; mm/hr), instantaneous wind speed (red contours; every 1 m/s), and mean sea level pressure (black contours; every 2 hPa) within ±10° of the cyclone center for all cyclones identified over eastern seaboard region in ERA5 between 1980 and 2009 (left column) and averaged across 12 RCMs (right column). Source: Pepler and Dowdy[178]

5.2.1.2 Projection

Surface and upper-level cyclones, and associated frontal systems, are projected to decline in frequency over southern Australia during the 21st century [178]. This signal is consistent between CMIP5 and RCMs and is reflected in the contraction of Southern Hemisphere storm track [181]. The average number of east coast lows are also projected to decrease in eastern Australia (Figure 24) [179]. The decline in cyclones is projected to have a significant impact on future mean rainfall, especially in regions that currently receive a large proportion of rainfall from cyclones (including NSW). Over 80% of southern Australia winter rainfall decline projections can be attributed to declining frequency in cyclones [178]. The decrease in cyclone frequency is mostly focussed in the winter over southern NSW (Figure 25), which currently receives up to 50% of winter rainfall from east coast lows [8,179].

During the warm summer, rainfall projections associated with deep cyclones and shallow cyclones counteract each other to result in minimal change. Total rainfall associated with deep cyclones (surface cyclone with upper level support) is projected to decline across southern Australia by 3.7mm per degree of warming, while shallow cyclone rainfall is projected to increase by 2.3mm per degree of warming [178].

Heavy rain days associated with cyclones are projected to increase along the eastern seaboard (+5% per degree of warming), with agreement of over 90% of RCMs [178]. The combination of decreased cyclone frequency but increased rainfall rate and cyclone intensity reflects a shift in the distribution of rainfall associated with cyclones across eastern and southern Australia [178]. Additionally, over 75% of RCMs simulate cyclones in 2070-99 with peak rainfall rates greater than any event in the 1980-2009 period [178]. This is important to consider in combination with historical and palaeoclimate evidence of events that are more extreme than experienced over the reanalysis observational period.

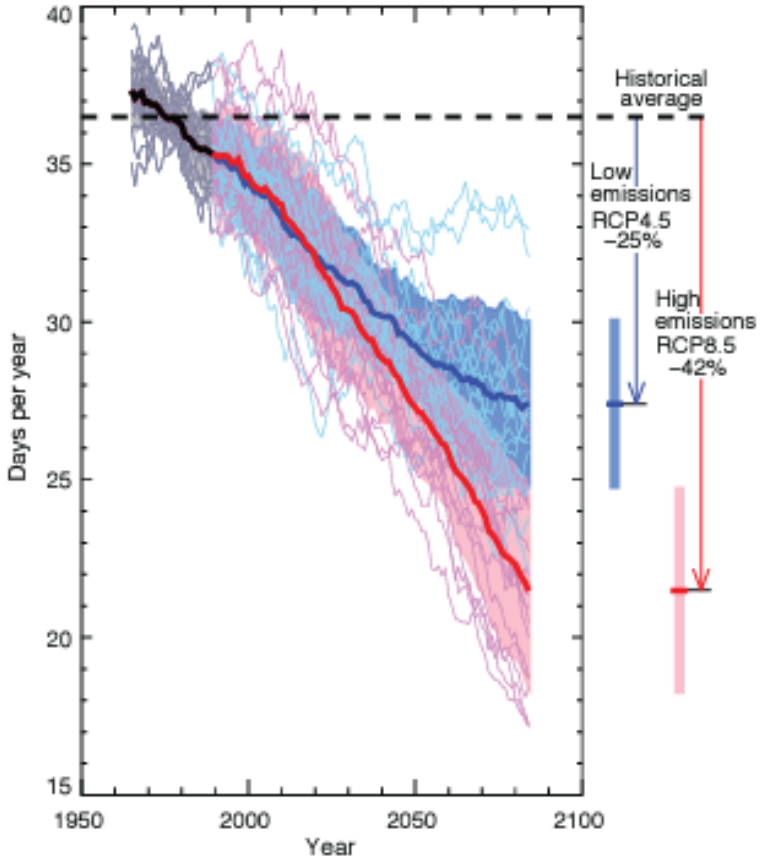

Figure 23: The number of days per year of east coast low events is projected to decline. Source: https://nespclimate.com.au/outreach-publications/

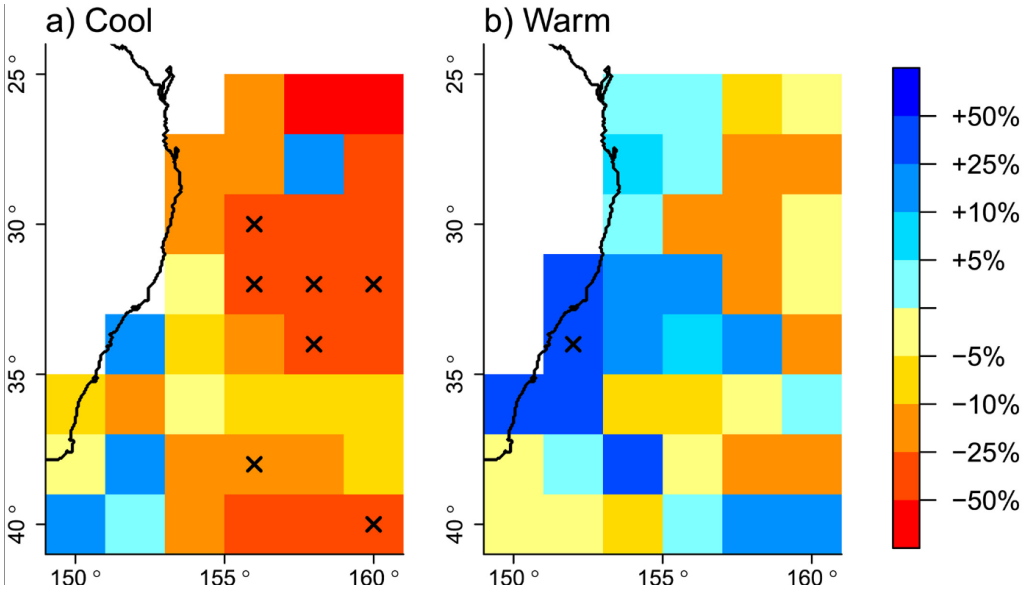

Figure 24: Median percentage change in east coast low frequency between 1990-2009 and 2060-2079 for a) cool season (May-October) and b) warm season (November to April). Source: Pepler et al.[179].

5.2.2 Atmospheric rivers

In the Australian region there are limited studies directly assessing the influence of atmospheric rivers on Australian rainfall [125,130]. The only model evaluation study focusses on the Sydney region [130].

5.2.2.1 Evaluation

Reid et al. (2021) evaluated the representation of atmospheric rivers in 16 CMIP6 models over the Sydney region using the integrated vapour transport (IVT) variable which is used to define atmospheric rivers (>250 Kg m^{-1} s^{-1}). Model IVT values less than the atmospheric river threshold displayed a negative bias in the CMIP6 historical runs. However, for IVT values that met atmospheric river thresholds, the CMIP6 models realistically simulated IVT conditions. The best performing model (EC-Earth3) only deviated from ERA5 observations by 15.5 Kg m^{-1} s^{-1}, while the worst performing model deviated by 130 Kg m^{-1} s^{-1} (BCC-CSM2-MR) [130].

Reid et al.[130] also indicated that climate sensitivity of models may influence IVT projections and atmospheric river detection. They found that models with faster rate of warming generally projected higher IVT increases.

5.2.2.2 Projection

CMIP6 models that simulate IVT over the Sydney region consistently with observations project an increased frequency of atmospheric rivers, particularly for event intensity greater than 300 Kg m^{-1} s^{-1} [130]. The frequency of multi-day high IVT events are also likely to increase under medium and high emission scenarios (i.e. SSP2-4.5 and SSP5-8.5). Generalised extreme modelling also estimated that the March 2021 atmospheric river event in Sydney would be become twice as likely in both medium and high emission scenarios [130]. The regional findings for Sydney are consistent with global analysis of atmospheric rivers, which found significant increases in the frequency and/or intensity of water vapour transport across mid-latitude regions of the Southern Hemisphere [187,188].

5.2.3 Anticyclones (high pressure systems)

Australian specific model evaluation studies related to anticyclones and their influence on rainfall projections is an active area of research.

5.2.3.1 Evaluation

CMIP5 models underestimate the observed frequency of anticyclones across the southern hemisphere, and within the Australian domain (Figure 26) [189]. The worst performing models, ACCESS and CNRM-CM5, underestimate anticyclone frequency by 30% compared to ERA5. However, the majority of models (with the exception of HadGem2-CC) simulate the spatial representation of peak anticyclone frequency within 2° of ERA5 reanalysis and capture the seasonality of the subtropical high-pressure belt (i.e. poleward migration in summer) [189]. Despite the frequency bias, CMIP5 models are able to simulate both quasi-stationary (e.g. Tasman sea blocking high pressure system) and mobile anticyclones [189].

In contrast RCM ensembles overestimate the observed frequency of anticyclones in the Australian domain, producing more than twice as many anticyclone centres per year than ERA5 reanalysis observations. This is likely due to higher spatial resolution generating multiple 'centres' within one larger anticyclone [189].

5.2.3.2 Projection

Minimal change in overall anticyclone frequency is projected for southeast Australia (140–150 °E, 30–40 °S) during May to October. However, a shift in distribution of type of anticyclone is projected with a decrease (-0.88 days per degree of warming) in quasi-stationary anticyclones and an increase (+0.94 days per degree of warming) in mobile anticyclones [189]. A decrease in quasi-stationary anticyclone frequency in the Tasman Sea region could influence rainfall in southeast NSW, by either blocking the passage of cold fronts into the region (reduced rainfall) or increasing the chance of onshore showers (increased rainfall).

Between November-April, CMIP5 models project a decrease in the frequency of anticyclones by 2070-2099, with both quasi-stationary and mobile anticyclones declining. GCMs project a decline of 1.4 days per degree of warming, while RCMs project a more rapid decline of 2 days per degree of warming. The projected decrease in quasi-stationary anticyclones may lead to less persistent moist onshore flow set ups during summer and autumn which often contribute to drought breaking rainfall in the region [3,111].

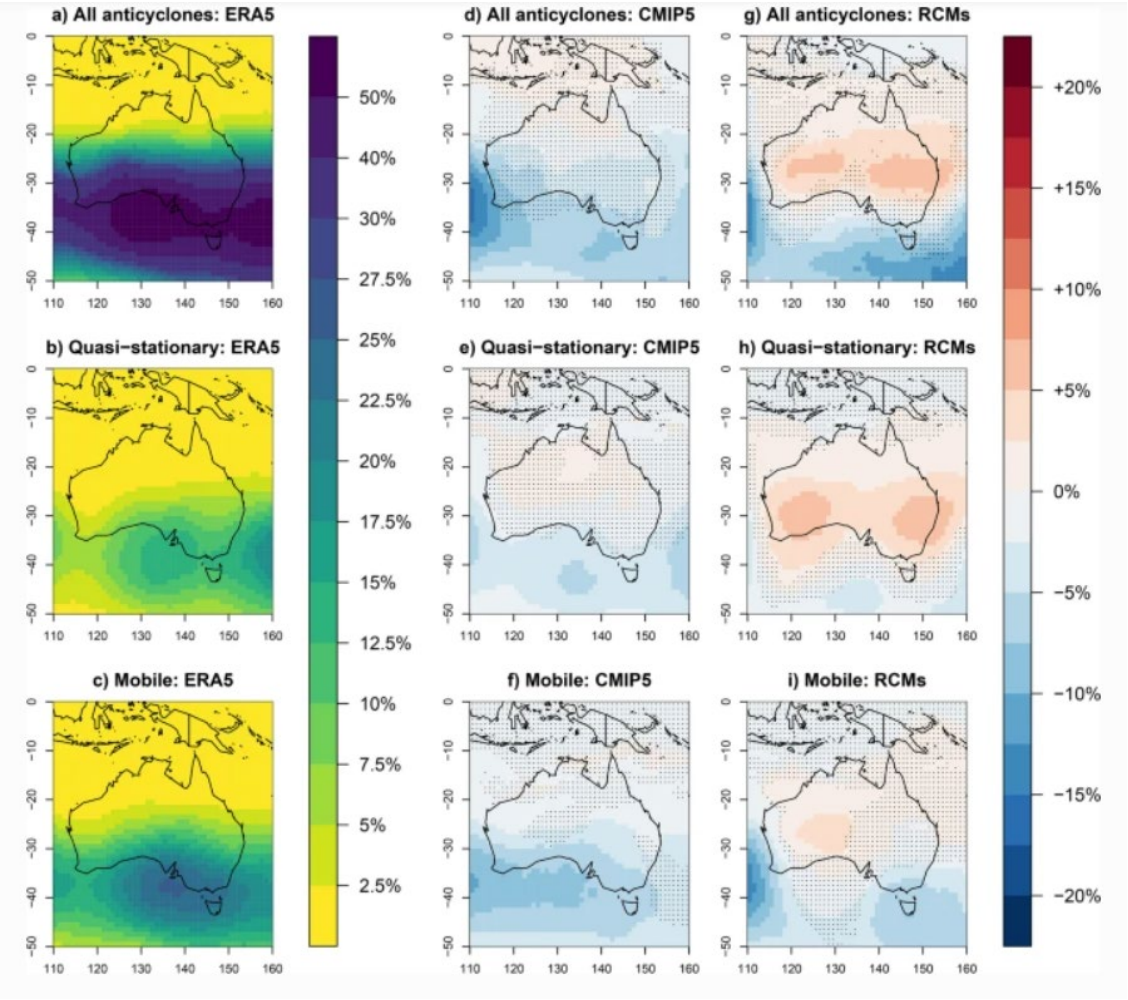

Figure 25: The percentage of anticyclone days (all, quasi-stationary and mobile) between 1980-2009 in reanalysis observations (ERA5) and ensemble mean model biases for CMIP5 and RCMs. Source: Pepler[189]

6 Conclusion

NSW rainfall is highly variable and influenced by a combination of factors across spatial and temporal scales, from synoptic weather and large-scale circulation to remote modes of climate variability and anthropogenic climate change. The frequency of synoptic weather systems that deliver rainfall to NSW are modulated by interactions between modes of climate variability and anthropogenic climate change. The seasonal-interannual interaction between ENSO, IOD, SAM and MJO phases can amplify or diminish the associated rainfall impacts across NSW. The rainfall influence associated with modes of climate variability also vary by season and region. For example, the influence of SAM shifts between winter and summer and IOD+ conditions have an opposing influence between inland and coastal NSW. Additionally, the phase of the IPO modulates the frequency and intensity of ENSO and SAM events on a decadal scale, with negative IPO favouring increased frequency and intensity of La Niña events and positive SAM conditions. IPO also influences the strength of the relationship between ENSO and IOD to NSW rainfall (strong during IPO negative, weak during IPO positive).

Over coastal and northeast inland NSW, surface onshore easterly winds increase moisture and leads to rainfall as the air parcel is uplifted over the Great Dividing Range. Weather and climate drivers that enhance the easterly wind strength and vertical uplift are associated with widespread rainfall (e.g. La Niña, SAM+, east coast lows, atmospheric rivers and Tasman Sea high blocking). Over southern inland NSW enhanced westerly surface winds associated with cold fronts and extra-tropical cyclones between May and October are associated with increased rainfall through orographic uplift on the western side of the Great Dividing Range. These weather systems are more likely during SAM- conditions.

Over the observational period (post 1900) there is no robust rainfall trend at an annual or summer scale across NSW. However, winter rainfall has been below average or lowest on record over the past two decades across most of NSW which has been linked to reduced rainfall associated with cold fronts and extra-tropical cyclones, as well as reduced frequency and shifts in location of these weather systems. This is particularly concerning for water availability in the southern NSW catchments which receive most of their rainfall in winter.

Currently climate models poorly represent the dynamics of the key modes of climate variability that influence NSW rainfall. Poor representation of the physical dynamics (e.g. cold bias in the Pacific Ocean or warm bias in the Indian Ocean) leads to underestimation or overestimation of the amplitude (i.e. intensity) and temporal (i.e. length of positive or negative phases) variability of the climate variability modes. Poor dynamic representation also causes biases in the rainfall teleconnection to NSW which influences regional rainfall projections. The overestimation of IOD amplitudes leads to a stronger rainfall decline signal over southern inland NSW, while the poor simulation of ENSO dynamics (e.g. cold tongue bias) influences the teleconnection to NSW climate and could lead to an increase or decrease in projected rainfall depending on the spatial offset. Additionally, the subset of models that credibly represent the spatial structure of one climate driver (e.g. IPO or ENSO) do not align with the models that represent another climate driver (e.g. IOD). This makes it difficult to assess the compound influence of climate drivers on NSW rainfall into the future.

The spatial scale of weather systems important for NSW rainfall influences the ability for climate models to simulate them. CMIP models are broadly able to capture the shape and structure of large extra-tropical cyclones and anticyclones. However, the frequency is underestimated for cyclones and overestimated for anticyclones which impacts NSW rainfall projections. The underestimation of cyclones and overestimation of anticyclones potentially leads to an amplified reduction in projected rainfall. However, the rainfall impact of overestimation of anticyclone frequency would be dependent on the location of the systems (i.e. if over the Tasman Sea could lead to increased rainfall along the NSW coast through enhanced moist easterly winds).

Smaller cyclones, including east coast lows, are poorly simulated in CMIP models due to the large spatial grid resolution of CMIP models (~200km) and short timescale of east coast lows (2-3 days). Dynamically downscaled regional climate models improve the representation, frequency and associated rainfall processes of cyclones and anticyclones in the NSW region. The frequency of east coast lows, extra-tropical cyclones and associated frontal systems are projected to decline in the winter. However, summer frequency and intense cyclones with heavier rainfall over the NSW coast are projected to increase. This reflects a shift in distribution, with less cyclone days overall but more intense cyclones with increased rainfall rate. It is important to consider the projected distribution shift in the context of historical and palaeoclimate evidence of extreme cyclonic events.

The overall frequency of anticyclones over southeast Australia is projected to have minimal change, however the number of quasi-stationary high-pressure systems (e.g. Tasman Sea blocking high) is projected to decrease. This could lead to decreased warm season rainfall over coastal NSW through less persistent moist onshore easterly winds which often contribute to drought breaking rainfall.

Rainfall projections for NSW are highly uncertain, with only a robust decreasing trend present for the southern inland NSW. This rainfall reduction is linked to reduced frequency and rainfall associated with cold fronts and extra-tropical cyclones which is driven by the poleward contraction of the storm track (represented by shift to positive SAM). However, the rainfall projections in other regions of NSW are likely impacted by the biases in how CMIP models represent the modes of climate variability and weather systems important for rainfall. It is vital to ensure that projected rainfall changes are associated with the correct mechanism and/or weather system. IPO plays a key climate role on the length of droughts and flood-dominated periods in NSW but the temporal variability is underestimated which results in the CMIP models being unable to simulate multi-decadal droughts or wet periods. Similarly, the misrepresentation of ENSO and IOD dynamics in CMIP models leads to the rainfall projection being amplified inaccurately through biases in the amplitude of extreme events (i.e. mean state shift to IOD+ causes reduced rainfall projections) and shifts in the teleconnection pathway (i.e. reduced ENSO impact on NSW rainfall). At a synoptic-weather scale, underestimation of extra-tropical cyclone frequency and overestimation of anticyclone frequency could lead to drier rainfall projections for southern NSW. Additionally, the structure, scale and associated rainfall with east coast lows are not represented by CMIP models which likely leads to drier projected mean conditions over coastal NSW.

7 References

1. Black, M. T. & Lane, T. P. An improved diagnostic for summertime rainfall along the eastern seaboard of Australia. *International Journal of Climatology* **35**, 4480–4492 (2015).
2. Twomey, C. R. & Kiem, A. S. Australian rainfall variability—Why is the eastern seaboard of Australia different to the rest of Australia and also internally inhomogeneous. *International Journal of Climatology* **41**, 5051–5071 (2021).
3. Udy, D. G., Vance, T. R., Kiem, A. S. & Holbrook, N. J. A synoptic bridge linking sea salt aerosol concentrations in East Antarctic snowfall to Australian rainfall. *Commun Earth Environ* **3**, 1–11 (2022).
4. Qi, L., Leslie, L. & Zhao, S. Cut-off low pressure systems over southern Australia: climatology and case study. *International Journal of Climatology: A Journal of the Royal Meteorological Society* **19**, 1633–1649 (1999).
5. Risbey, J. S., Pook, M. J., McIntosh, P. C., Wheeler, M. C. & Hendon, H. H. On the Remote Drivers of Rainfall Variability in Australia. *Monthly Weather Review* **137**, 3233–3253 (2009).
6. Speer, M. S., Wiles, P. & Pepler, A. Low pressure systems off the New South Wales coast and associated hazardous weather: establishment of a database. *Australian Meteorological and Oceanographic Journal* **58**, 29 (2009).
7. Pepler, A. S. *et al.* The contributions of fronts, lows and thunderstorms to southern Australian rainfall. *Climate Dynamics* **55**, 1489–1505 (2020).
8. Pepler, A., Coutts-Smith, A. & Timbal, B. The role of East Coast Lows on rainfall patterns and inter-annual variability across the East Coast of Australia. *International Journal of Climatology* **34**, 1011–1021 (2014).
9. Pepler, A., Hope, P. & Dowdy, A. Long-term changes in southern Australian anticyclones and their impacts. *Climate Dynamics* **53**, 4701–4714 (2019).
10. Bureau of Meteorology. Previous droughts. http://www.bom.gov.au/climate/drought/knowledge-centre/previous-droughts.shtml (2020).
11. Freund, M., Henley, B. J., Karoly, D. J., Allen, K. J. & Baker, P. J. Multi-century cool- and warm-season rainfall reconstructions for Australia's major climatic regions. *Climate of the Past* **13**, 1751–1770 (2017).
12. Kiem, A. S. *et al.* Natural hazards in Australia: droughts. *Climatic Change* **139**, 37–54 (2016).
13. King, A. D., Pitman, A. J., Henley, B. J., Ukkola, A. M. & Brown, J. R. The role of climate variability in Australian drought. *Nature Climate Change* **10**, 177–179 (2020).
14. van Dijk, A. I. J. M. *et al.* The Millennium Drought in southeast Australia (2001–2009): Natural and human causes and implications for water resources, ecosystems, economy, and society. *Water Resources Research* **49**, 1040–1057 (2013).
15. Ashcroft, L., Gergis, J. & Karoly, D. J. A historical climate dataset for southeastern Australia, 1788–1859. *Geoscience Data Journal* **1**, 158–178 (2014).
16. Gallant, A. J. E. & Gergis, J. An experimental streamflow reconstruction for the River Murray, Australia, 1783-1988. *Water Resources Research* **47**, (2011).
17. Ho, M., Kiem, A. S. & Verdon-Kidd, D. C. A paleoclimate rainfall reconstruction in the Murray-Darling Basin (MDB), Australia: 2. Assessing hydroclimatic risk using paleoclimate records of wet and dry epochs. *Water Resources Research* **51**, 8380–8396 (2015).
18. Ho, M., Kiem, A. S. & Verdon-Kidd, D. C. A paleoclimate rainfall reconstruction in the Murray-Darling Basin (MDB), Australia: 1. Evaluation of different paleoclimate archives, rainfall networks, and reconstruction techniques. *Water Resources Research* **51**, 8362–8379 (2015).
19. Kiem, A. S. & Franks, S. W. Multi-decadal variability of drought risk, eastern Australia. *Hydrological Processes* **18**, 2039–2050 (2004).
20. Verdon-Kidd, D. C. & Kiem, A. S. Quantifying Drought Risk in a Nonstationary Climate. *Journal of Hydrometeorology* **11**, 1019–1031 (2010).

21. Flack, A. L., Kiem, A. S., Vance, T. R., Tozer, C. R. & Roberts, J. L. Comparison of published palaeoclimate records suitable for reconstructing annual to sub-decadal hydroclimatic variability in eastern Australia: implications for water resource management and planning. *Hydrol. Earth Syst. Sci.* **24**, 5699–5712 (2020).

22. Kiem, A. S. *et al.* Learning from the past – Using palaeoclimate data to better understand and manage drought in South East Queensland (SEQ), Australia. *Journal of Hydrology: Regional Studies* **29**, 100686 (2020).

23. Kiem, A. S., Franks, S. W. & Kuczera, G. Multi-decadal variability of flood risk. *Geophysical Research Letters* **30**, (2003).

24. Steiger, N. J., Smerdon, J. E., Cook, E. R. & Cook, B. I. A reconstruction of global hydroclimate and dynamical variables over the Common Era. *Scientific Data* **5**, 180086 (2018).

25. Heinrich, I. & Allen, K. Current Issues and Recent Advances in Australian Dendrochronology: Where to Next? *Geographical Research* **51**, 180–191 (2013).

26. Croke, J. *et al.* A palaeoclimate proxy database for water security planning in Queensland Australia. *Sci Data* **8**, 292 (2021).

27. O'Donnell, A. J., McCaw, W. L., Cook, E. R. & Grierson, P. F. Megadroughts and pluvials in southwest Australia: 1350–2017 CE. *Clim Dyn* **57**, 1817–1831 (2021).

28. Palmer, J. G. *et al.* Drought variability in the eastern Australia and New Zealand summer drought atlas (ANZDA, CE 1500–2012) modulated by the Interdecadal Pacific Oscillation. *Environmental Research Letters* **10**, (2015).

29. Lough, J. M. Great Barrier Reef coral luminescence reveals rainfall variability over northeastern Australia since the 17th century. *Paleoceanography* **26**, (2011).

30. Walter, R. M. *et al.* The CoralHydro2k database: a global, actively curated compilation of coral proxy records of tropical ocean hydrology and temperature for the Common Era. *Earth System Science Data* **15**, 2081–2116 (2023).

31. Barr, C. *et al.* Holocene El Niño–Southern Oscillation variability reflected in subtropical Australian precipitation. *Scientific Reports* **9**, 1627 (2019).

32. Barr, C. *et al.* Climate variability in south-eastern Australia over the last 1500 years inferred from the high-resolution diatom records of two crater lakes. *Quaternary Science Reviews* **95**, 115–131 (2014).

33. Dixon, B. C. *et al.* Low-resolution Australasian palaeoclimate records of the last 2000 years. *Climate of the Past* **13**, 1403–1433 (2017).

34. Tozer, C. R. *et al.* Reconstructing pre-instrumental streamflow in Eastern Australia using a water balance approach. *Journal of Hydrology* **558**, 632–646 (2018).

35. Tozer, C. R. *et al.* An ice core derived 1013-year catchment-scale annual rainfall reconstruction in subtropical eastern Australia. *Hydrology and Earth System Sciences* **20**, 1703–1717 (2016).

36. Vance, T. R., Roberts, J. L., Plummer, C. T., Kiem, A. S. & van Ommen, T. D. Interdecadal Pacific variability and eastern Australian megadroughts over the last millennium. *Geophysical Research Letters* **42**, 129–137 (2015).

37. Vance, T. R., van Ommen, T. D., Curran, M. A. J., Plummer, C. T. & Moy, A. D. A Millennial Proxy Record of ENSO and Eastern Australian Rainfall from the Law Dome Ice Core, East Antarctica. *Journal of Climate* **26**, 710–725 (2013).

38. Zhang, L., Kuczera, G., Kiem, A. S. & Willgoose, G. Using paleoclimate reconstructions to analyse hydrological epochs associated with Pacific decadal variability. *Hydrology and Earth System Sciences* **22**, 6399–6414 (2018).

39. Nicholls, N. Local and remote causes of the southern Australian autumn-winter rainfall decline, 1958–2007. *Climate dynamics* **34**, 835–845 (2010).

40. Power, S., Casey, T., Folland, C., Colman, A. & Mehta, V. Inter-decadal modulation of the impact of ENSO on Australia. *Climate Dynamics* **15**, 319–324 (1999).

41. Mann, M. E., Steinman, B. A. & Miller, S. K. Absence of internal multidecadal and interdecadal oscillations in climate model simulations. *Nat Commun* **11**, 49 (2020).

42. Vance, T. R. *et al.* Pacific decadal variability over the last 2000 years and implications for climatic risk. *Commun Earth Environ* **3**, 1–9 (2022).

43. Buckley, B. M. *et al.* Interdecadal Pacific Oscillation reconstructed from trans-Pacific tree rings: 1350–2004 CE. *Clim Dyn* **53**, 3181–3196 (2019).

44. Porter, S. E., Mosley-Thompson, E., Thompson, L. G. & Wilson, A. B. Reconstructing an Interdecadal Pacific Oscillation Index from a Pacific Basin–Wide Collection of Ice Core Records. *Journal of Climate* **34**, 3839–3852 (2021).

45. Henley, B. J. *et al.* A Tripole Index for the Interdecadal Pacific Oscillation. *Clim Dyn* **45**, 3077–3090 (2015).

46. Folland, C. K., Parker, D. E., Colman, A. W. & Washington, R. Large Scale Modes of Ocean Surface Temperature Since the Late Nineteenth Century. in *Beyond El Niño: Decadal and Interdecadal Climate Variability* (ed. Navarra, A.) 73–102 (Springer, 1999). doi:10.1007/978-3-642-58369-8_4.

47. MacDonald, G. M. & Case, R. A. Variations in the Pacific Decadal Oscillation over the past millennium. *Geophysical Research Letters* **32**, (2005).

48. Mann, M. E. *et al.* Global Signatures and Dynamical Origins of the Little Ice Age and Medieval Climate Anomaly. *Science* **326**, 1256–1260 (2009).

49. Rimbu, N., Ionita, M. & Lohmann, G. Interdecadal Pacific Oscillation in Northern Greenland Dust Concentration Variability During the Last 400 Years. *Geophysical Research Letters* **49**, e2022GL101500 (2022).

50. D'Arrigo, R., Cook, E. R., Wilson, R. J., Allan, R. & Mann, M. E. On the variability of ENSO over the past six centuries. *Geophysical Research Letters* **32**, (2005).

51. Deser, C., Alexander, M. A., Xie, S.-P. & Phillips, A. S. Sea Surface Temperature Variability: Patterns and Mechanisms. *Annual Review of Marine Science* **2**, 115–143 (2010).

52. McPhaden, M. J., Lee, T., Fournier, S. & Balmaseda, M. A. ENSO Observations. in *El Niño Southern Oscillation in a Changing Climate* 39–63 (2020).

53. Pepler, A., Timbal, B., Rakich, C. & Coutts-Smith, A. Indian Ocean Dipole Overrides ENSO's Influence on Cool Season Rainfall across the Eastern Seaboard of Australia. *Journal of Climate* **27**, 3816–3826 (2014).

54. Power, S., Haylock, M., Colman, R. & Wang, X. Asymmetry in the Australian response to ENSO and the predictability of inter-decadal changes in ENSO teleconnections. (2005).

55. Cai, W., Rensch, P. van, Cowan, T. & Sullivan, A. Asymmetry in ENSO Teleconnection with Regional Rainfall, Its Multidecadal Variability, and Impact. *Journal of Climate* **23**, 4944–4955 (2010).

56. Chung, C. T. Y. & Power, S. B. The non-linear impact of El Nino, La Nina and the Southern Oscillation on seasonal and regional Australian precipitation. *JSHESS* **67**, 25–45 (2017).

57. King, A. D., Donat, M. G., Alexander, L. V. & Karoly, D. J. The ENSO-Australian rainfall teleconnection in reanalysis and CMIP5. *Clim Dyn* **44**, 2623–2635 (2015).

58. van Rensch, P., Gallant, A. J. E., Cai, W. & Nicholls, N. Evidence of local sea surface temperatures overriding the southeast Australian rainfall response to the 1997–1998 El Niño. *Geophysical Research Letters* **42**, 9449–9456 (2015).

59. Brown, J. N., McIntosh, P. C., Pook, M. J. & Risbey, J. S. An Investigation of the Links between ENSO Flavors and Rainfall Processes in Southeastern Australia. *Monthly Weather Review* **137**, 3786–3795 (2009).

60. Wang, G. & Hendon, H. H. Sensitivity of Australian Rainfall to Inter–El Niño Variations. *Journal of Climate* **20**, 4211–4226 (2007).

61. Freund, M. B., Marshall, A. G., Wheeler, M. C. & Brown, J. N. Central Pacific El Niño as a Precursor to Summer Drought-Breaking Rainfall Over Southeastern Australia. *Geophysical Research Letters* **48**, e2020GL091131 (2021).

62. Cobb, K. M., Charles, C. D., Cheng, H. & Edwards, R. L. El Niño/Southern Oscillation and tropical Pacific climate during the last millennium. *Nature* **424**, 271–276 (2003).

63. Conroy, J. L. *et al.* Unprecedented recent warming of surface temperatures in the eastern tropical Pacific Ocean. *Nature Geosci* **2**, 46–50 (2009).

64. Meyerson, E. A. *et al.* The polar expression of ENSO and sea-ice variability as recorded in a South Pole ice core. *Annals of Glaciology* **35**, 430–436 (2002).

65. Crockart, C. K. *et al.* El Niño–Southern Oscillation signal in a new East Antarctic ice core, Mount Brown South. *Clim. Past* **17**, 1795–1818 (2021).

66. Barrett, H. G., Jones, J. M. & Bigg, G. R. Reconstructing El Niño Southern Oscillation using data from ships' logbooks, 1815–1854. Part II: Comparisons with existing ENSO reconstructions and implications for reconstructing ENSO diversity. *Clim Dyn* **50**, 3131–3152 (2018).

67. Saji, N. H., Goswami, B. N., Vinayachandran, P. N. & Yamagata, T. A dipole mode in the tropical Indian Ocean. *Nature* **401**, 360–363 (1999).

68. Saji, N. & Yamagata, T. Possible impacts of Indian Ocean dipole mode events on global climate. *Climate Research* **25**, 151–169 (2003).

69. Webster, P. J., Moore, A. M., Loschnigg, J. P. & Leben, R. R. Coupled ocean–atmosphere dynamics in the Indian Ocean during 1997–98. *Nature* **401**, 356–360 (1999).

70. Abram, N. J. *et al.* Palaeoclimate perspectives on the Indian Ocean Dipole. *Quaternary Science Reviews* **237**, 106302 (2020).

71. Ashok, K., Guan, Z. & Yamagata, T. Influence of the Indian Ocean Dipole on the Australian winter rainfall. *Geophysical Research Letters* **30**, (2003).

72. Nicholls, N. Sea surface temperatures and Australian winter rainfall. *Journal of Climate* **2**, 965–973 (1989).

73. Ummenhofer, C. C. *et al.* What causes southeast Australia's worst droughts? *Geophysical Research Letters* **36**, (2009).

74. Verdon, D. C. & Franks, S. W. Indian Ocean sea surface temperature variability and winter rainfall: Eastern Australia. *Water Resources Research* **41**, (2005).

75. Verdon-Kidd, D. C. On the classification of different flavours of Indian Ocean Dipole events. *International Journal of Climatology* **38**, 4924–4937 (2018).

76. Abram, N. J., Gagan, M. K., Cole, J. E., Hantoro, W. S. & Mudelsee, M. Recent intensification of tropical climate variability in the Indian Ocean. *Nature Geosci* **1**, 849–853 (2008).

77. Bureau of Meteorology. Indian Ocean climate influences. http://www.bom.gov.au/climate/iod/ (2022).

78. Lim, E.-P. & Hendon, H. H. Causes and predictability of the negative Indian Ocean Dipole and its impact on La Niña during 2016. *Scientific reports* **7**, 1–11 (2017).

79. Fogt, R. L., Jones, J. M. & Renwick, J. Seasonal Zonal Asymmetries in the Southern Annular Mode and Their Impact on Regional Temperature Anomalies. *Journal of Climate* **25**, 6253–6270 (2012).

80. Marshall, G. J. Trends in the Southern Annular Mode from observations and reanalyses. *Journal of climate* **16**, 4134–4143 (2003).

81. Campitelli, E., Díaz, L. B. & Vera, C. Assessment of zonally symmetric and asymmetric components of the Southern Annular Mode using a novel approach. *Clim Dyn* **58**, 161–178 (2022).

82. Udy, D. G., Vance, T. R., Kiem, A. S., Holbrook, N. J. & Curran, M. A. J. Links between Large-Scale Modes of Climate Variability and Synoptic Weather Patterns in the Southern Indian Ocean. *Journal of Climate* **34**, 883–899 (2021).

83. Boschat, G., Purich, A., Rudeva, I. & Arblaster, J. Impact of zonal and meridional atmospheric flow on surface climate and extremes in the Southern Hemisphere. *Journal of Climate* **1**, 1–45 (2023).

84. Arblaster, J. M., Meehl, G. A. & Karoly, D. J. Future climate change in the Southern Hemisphere: Competing effects of ozone and greenhouse gases. *Geophysical Research Letters* **38**, (2011).

85. Thompson, D. W. J. & Solomon, S. Interpretation of Recent Southern Hemisphere Climate Change. *Science* **296**, 895–899 (2002).

86. Nguyen, H., Lucas, C., Evans, A., Timbal, B. & Hanson, L. Expansion of the Southern Hemisphere Hadley cell in response to greenhouse gas forcing. *Journal of Climate* **28**, 8067–8077 (2015).

87. Hersbach, H. *et al.* The ERA5 global reanalysis. *Quarterly Journal of the Royal Meteorological Society* **146**, 1999–2049 (2020).

88. Pezza, A. B., Rashid, H. A. & Simmonds, I. Climate links and recent extremes in antarctic sea ice, high-latitude cyclones, Southern Annular Mode and ENSO. *Climate Dynamics* **38**, 57–73 (2012).

89. Hendon, H. H., Thompson, D. W. & Wheeler, M. C. Australian rainfall and surface temperature variations associated with the Southern Hemisphere annular mode. *Journal of Climate* **20**, 2452–2467 (2007).

90. Ho, M., Kiem, A. S. & Verdon-Kidd, D. C. The Southern Annular Mode: a comparison of indices. *Hydrol. Earth Syst. Sci.* **16**, 967–982 (2012).

91. Gillett, N. P., Kell, T. D. & Jones, P. Regional climate impacts of the Southern Annular Mode. *Geophysical Research Letters* **33**, (2006).

92. Lim, E.-P. *et al.* Australian hot and dry extremes induced by weakenings of the stratospheric polar vortex. *Nature Geoscience* **12**, 896–901 (2019).

93. Abram, N. J. *et al.* Connections of climate change and variability to large and extreme forest fires in southeast Australia. *Communications Earth & Environment* **2**, 8 (2021).

94. Fiddes, S. L., Pezza, A. B. & Renwick, J. Significant extra-tropical anomalies in the lead up to the Black Saturday fires. *International Journal of Climatology* **36**, 1011–1018 (2016).

95. Madden, R. A. & Julian, P. R. Observations of the 40–50-Day Tropical Oscillation—A Review. *Monthly Weather Review* **122**, 814–837 (1994).

96. Schwendike, J., Berry, G. J., Fodor, K. & Reeder, M. J. On the Relationship Between the Madden-Julian Oscillation and the Hadley and Walker Circulations. *Journal of Geophysical Research: Atmospheres* **126**, e2019JD032117 (2021).

97. Zhang, C. Madden-Julian Oscillation. *Reviews of Geophysics* **43**, (2005).

98. Cowan, T., Wheeler, M. C. & Marshall, A. G. The Combined Influence of the Madden–Julian Oscillation and El Niño–Southern Oscillation on Australian Rainfall. *Journal of Climate* **36**, 313–334 (2022).

99. Wheeler, M. C., Hendon, H. H., Cleland, S., Meinke, H. & Donald, A. Impacts of the Madden–Julian Oscillation on Australian Rainfall and Circulation. *Journal of Climate* **22**, 1482–1498 (2009).

100. Wheeler, M. C. & Hendon, H. H. An All-Season Real-Time Multivariate MJO Index: Development of an Index for Monitoring and Prediction. *Monthly Weather Review* **132**, 1917–1932 (2004).

101. Borowiak, A., King, A. & Lane, T. The Link Between the Madden-Julian Oscillation and Rainfall Trends in Northwest Australia. *Geophysical Research Letters* **50**, e2022GL101799 (2023).

102. Yan, H. *et al.* The first detection of the Madden-Julian Oscillation signal in daily to hourly resolution proxy records derived from a natural archive of Giant Clam Shell (Tridacna spp.). *Earth and Planetary Science Letters* **555**, 116703 (2021).

103. Yang, D. *et al.* Role of Tropical Variability in Driving Decadal Shifts in the Southern Hemisphere Summertime Eddy-Driven Jet. *Journal of Climate* **33**, 5445–5463 (2020).

104. Weir, T. *et al.* Interdecadal modulation of the effect of ENSO on rainfall in the southwestern Pacific. *JSHESS* **71**, 53–65 (2021).

105. Ashok, K., Guan, Z. & Yamagata, T. A look at the relationship between the ENSO and the Indian Ocean dipole. *Journal of the Meteorological Society of Japan. Ser. II* **81**, 41–56 (2003).

106. Bureau of Meteorology. The recent climate – news reports and summaries. http://www.bom.gov.au/climate/current/ (2023).

107. Lim, E.-P. *et al.* Why Australia was not wet during spring 2020 despite La Niña. *Scientific reports* **11**, 1–15 (2021).

108. Abram, N. J. *et al.* Evolution of the Southern Annular Mode during the past millennium. *Nature Climate Change* **4**, 564–569 (2014).

109. Dätwyler, C., Grosjean, M., Steiger, N. J. & Neukom, R. Teleconnections and relationship between the El Niño–Southern Oscillation (ENSO) and the Southern Annular Mode (SAM) in reconstructions and models over the past millennium. *Climate of the Past* **16**, 743–756 (2020).

110. Fogt, R. L., Bromwich, D. H. & Hines, K. M. Understanding the SAM influence on the South Pacific ENSO teleconnection. *Climate Dynamics* **36**, 1555–1576 (2011).

111. Holgate, C. M., Van Dijk, A. I. J. M., Evans, J. P. & Pitman, A. J. Local and Remote Drivers of Southeast Australian Drought. *Geophysical Research Letters* **47**, e2020GL090238 (2020).

112. Taschetto, A. S. & England, M. H. An analysis of late twentieth century trends in Australian rainfall. *International Journal of Climatology* **29**, 791–807 (2009).

113. Cai, D., Abram, N. J., Sharples, J. J. & Perkins-Kirkpatrick, S. E. Increasing intensity and frequency of cold fronts contributed to Australia's 2019–2020 Black Summer fire disaster. *Environmental Research Letters* **17**, 094044 (2022).

114. Dowdy, A. J. *et al.* Review of Australian east coast low pressure systems and associated extremes. *Climate Dynamics* **53**, 4887–4910 (2019).

115. Gray, J. L. *et al.* Characterizing Australia's east coast cyclones (1950–2019). *International Journal of Climatology* **n/a**, (2023).

116. Kiem, A. S. *et al.* Links between East Coast Lows and the spatial and temporal variability of rainfall along the eastern seaboard of Australia. *Journal of Southern Hemisphere Earth Systems Science* **66**, 162–176 (2016).

117. Browning, S. A. & Goodwin, I. D. Large-scale drivers of Australian east coast cyclones since 1851. *JSHESS* **66**, 125–151 (2016).

118. Pepler, A. S. & Rakich, C. S. Extreme inflow events and synoptic forcing in Sydney catchments. in vol. 11 012010 (IOP Publishing, 2010).

119. Gray, J. *et al.* A comparison of the MATCHES and NCEP1 databases for use in Australian east coast low studies. *Weather and Climate Extremes* **34**, 100400 (2021).

120. Catto, J. L., Jakob, C., Berry, G. & Nicholls, N. Relating global precipitation to atmospheric fronts. *Geophysical Research Letters* **39**, (2012).

121. Sturman, A. P. & Tapper, N. J. *The weather and climate of Australia and New Zealand*. (Oxford University Press, USA, 1996).

122. Pook, M. *et al.* The autumn break for cropping in southeast Australia: trends, synoptic influences and impacts on wheat yield. *International Journal of Climatology* **29**, 2012–2026 (2009).

123. Pepler, A. S., Dowdy, A. J. & Hope, P. The differing role of weather systems in southern Australian rainfall between 1979–1996 and 1997–2015. *Clim Dyn* **56**, 2289–2302 (2021).

124. Ralph, F. M., Dettinger, M. D., Cairns, M. M., Galarneau, T. J. & Eylander, J. Defining "atmospheric river": How the Glossary of Meteorology helped resolve a debate. *Bulletin of the American Meteorological Society* **99**, 837–839 (2018).

125. Reid, K. J., King, A. D., Lane, T. P. & Hudson, D. Tropical, Subtropical, and Extratropical Atmospheric Rivers in the Australian Region. *Journal of Climate* **35**, 2697–2708 (2022).

126. Gorodetskaya, I. V. *et al.* The role of atmospheric rivers in anomalous snow accumulation in East Antarctica. *Geophysical Research Letters* **41**, 6199–6206 (2014).

127. Kingston, D. G., Lavers, D. A. & Hannah, D. M. Floods in the Southern Alps of New Zealand: the importance of atmospheric rivers. *Hydrological Processes* **30**, 5063–5070 (2016).

128. Lavers, D. A. *et al.* Winter floods in Britain are connected to atmospheric rivers. *Geophysical Research Letters* **38**, (2011).

129. Lavers, D. A. & Villarini, G. Atmospheric rivers and flooding over the central United States. *Journal of Climate* **26**, 7829–7836 (2013).

130. Reid, K. J., O'Brien, T. A., King, A. D. & Lane, T. P. Extreme Water Vapor Transport During the March 2021 Sydney Floods in the Context of Climate Projections. *Geophysical Research Letters* **48**, e2021GL095335 (2021).

131. Wille, J. D. *et al.* Antarctic atmospheric river climatology and precipitation impacts. *Journal of Geophysical Research: Atmospheres* **126**, e2020JD033788 (2021).

132. Pook, M. Atmosphere blocking in the Australiasian region in the Southern Hemisphere winter. (University of Tasmania, Hobart, Tasmania, Australia, 1994).

133. Coughlan, M. J. A comparative climatology of blocking action in the two hemispheres. *Aust. Meteor. Mag.* **31**, 3–13 (1983).

134. M. J. Pook *et al.* The Seasonal Cycle of Blocking and Associated Physical Mechanisms in the Australian Region and Relationship with Rainfall. *Monthly Weather Review* **141**, 4534–4553 (2013).

135. Scarchilli, C., Frezzotti, M. & Ruti, P. M. Snow precipitation at four ice core sites in East Antarctica: provenance, seasonality and blocking factors. *Climate Dynamics* **37**, 2107–2125 (2011).

136. Risbey, J. S., McIntosh, P. C. & Pook, M. J. Synoptic components of rainfall variability and trends in southeast Australia. *International Journal of Climatology* **33**, 2459–2472 (2013).

137. Pook, M. J., Risbey, J. S. & McIntosh, P. C. A comparative synoptic climatology of cool-season rainfall in major grain-growing regions of southern Australia. *Theoretical and applied climatology* **117**, 521–533 (2014).

138. Risbey, J. S., Pook, M. J., McIntosh, P. C., Ummenhofer, C. C. & Meyers, G. Characteristics and variability of synoptic features associated with cool season rainfall in southeastern Australia. *International Journal of Climatology: A Journal of the Royal Meteorological Society* **29**, 1595–1613 (2009).

139. Cai, W., Rensch, P. van, Cowan, T. & Hendon, H. H. Teleconnection Pathways of ENSO and the IOD and the Mechanisms for Impacts on Australian Rainfall. *Journal of Climate* **24**, 3910–3923 (2011).

140. Meyers, G., McIntosh, P., Pigot, L. & Pook, M. The Years of El Niño, La Niña, and Interactions with the Tropical Indian Ocean. *Journal of Climate* **20**, 2872–2880 (2007).

141. McKay, R. C. *et al.* Can southern Australian rainfall decline be explained? A review of possible drivers. *WIREs Climate Change* **14**, e820 (2023).

142. Pepler, A., Coutts-Smith, A. & Timbal, B. The role of East Coast Lows on rainfall patterns and inter-annual variability across the East Coast of Australia. *International Journal of Climatology* **34**, 1011–1021 (2014).

143. Black, M. T. & Lane, T. P. An improved diagnostic for summertime rainfall along the eastern seaboard of Australia. *International Journal of Climatology* **35**, 4480–4492 (2015).

144. Henley, B. J. *et al.* Spatial and temporal agreement in climate model simulations of the Interdecadal Pacific Oscillation. *Environ. Res. Lett.* **12**, 044011 (2017).

145. Fasullo, J. T., Phillips, A. S. & Deser, C. Evaluation of Leading Modes of Climate Variability in the CMIP Archives. *Journal of Climate* **33**, 5527–5545 (2020).

146. Ma, Y., Yuan, N., Dong, T. & Dong, W. On the Pacific Decadal Oscillation Simulations in CMIP6 Models: A New Test-Bed from Climate Network Analysis. *Asia-Pac J Atmos Sci* **59**, 17–28 (2023).

147. Di Virgilio, G. *et al.* Selecting CMIP6 GCMs for CORDEX Dynamical Downscaling: Model Performance, Independence, and Climate Change Signals. *Earth's Future* **10**, e2021EF002625 (2022).

148. Grose, M. R. *et al.* Insights From CMIP6 for Australia's Future Climate. *Earth's Future* **8**, e2019EF001469 (2020).

149. Folland, C., Renwick, J., Salinger, M. & Mullan, A. Relative influences of the interdecadal Pacific oscillation and ENSO on the South Pacific convergence zone. *Geophysical Research Letters* **29**, 21–1 (2002).

150. Kociuba, G. & Power, S. B. Inability of CMIP5 models to simulate recent strengthening of the Walker circulation: Implications for projections. *Journal of Climate* **28**, 20–35 (2015).

151. Lee, J. *et al.* Future Global Climate: Scenario-Based Projections and Near-Term Information. in *Climate Change 2021: The Physical Science Basis. Contribution of Working Group I to the Sixth Assessment Report of the Intergovernmental Panel on Climate Change [Masson-Delmotte, V., P. Zhai, A. Pirani, S.L. Connors, C. Péan, S. Berger, N. Caud, Y. Chen, L. Goldfarb, M.I. Gomis, M. Huang, K. Leitzell, E. Lonnoy, J.B.R. Matthews, T.K. Maycock, T. Waterfield, O. Yelekçi, R. Yu, and B. Zhou (eds.)]* 553–672 (Cambridge University Press, 2021).

152. Beobide-Arsuaga, G., Bayr, T., Reintges, A. & Latif, M. Uncertainty of ENSO-amplitude projections in CMIP5 and CMIP6 models. *Clim Dyn* **56**, 3875–3888 (2021).

153. McGregor, S., Cassou, C., Kosaka, Y. & Phillips, A. S. Projected ENSO Teleconnection Changes in CMIP6. *Geophysical Research Letters* **49**, e2021GL097511 (2022).

154. Jiang, W., Huang, P., Huang, G. & Ying, J. Origins of the Excessive Westward Extension of ENSO SST Simulated in CMIP5 and CMIP6 Models. *Journal of Climate* **34**, 2839–2851 (2021).

155. Cai, W. *et al.* Anthropogenic impacts on twentieth-century ENSO variability changes. *Nat Rev Earth Environ* 1–12 (2023) doi:10.1038/s43017-023-00427-8.

156. Cai, W. *et al.* Changing El Niño–Southern Oscillation in a warming climate. *Nat Rev Earth Environ* **2**, 628–644 (2021).

157. Cai, W. *et al.* Increased ENSO sea surface temperature variability under four IPCC emission scenarios. *Nat. Clim. Chang.* **12**, 228–231 (2022).

158. Cai, W. & Cowan, T. Why is the amplitude of the Indian Ocean Dipole overly large in CMIP3 and CMIP5 climate models? *Geophysical Research Letters* **40**, 1200–1205 (2013).

159. Weller, E. & Cai, W. Realism of the Indian Ocean Dipole in CMIP5 Models: The Implications for Climate Projections. *Journal of Climate* **26**, 6649–6659 (2013).

160. Zheng, X.-T. *et al.* Indian Ocean Dipole Response to Global Warming in the CMIP5 Multimodel Ensemble. *Journal of Climate* **26**, 6067–6080 (2013).

161. McKenna, S., Santoso, A., Gupta, A. S., Taschetto, A. S. & Cai, W. Indian Ocean Dipole in CMIP5 and CMIP6: characteristics, biases, and links to ENSO. *Scientific Reports* **10**, 11500 (2020).

162. Cai, W. *et al.* Stabilised frequency of extreme positive Indian Ocean Dipole under 1.5 °C warming. *Nat Commun* **9**, 1419 (2018).

163. Cai, W. *et al.* Increased frequency of extreme Indian Ocean Dipole events due to greenhouse warming. *Nature* **510**, 254–258 (2014).

164. Zhang, X. *et al.* Evaluation of the seasonality and spatial aspects of the Southern Annular Mode in CMIP6 models. *International Journal of Climatology* **42**, 3820–3837 (2022).

165. Zheng, F., Li, J., Clark, R. T. & Nnamchi, H. C. Simulation and Projection of the Southern Hemisphere Annular Mode in CMIP5 Models. *Journal of Climate* **26**, 9860–9879 (2013).

166. Morgenstern, O. The Southern Annular Mode in 6th Coupled Model Intercomparison Project Models. *Journal of Geophysical Research: Atmospheres* **126**, e2020JD034161 (2021).

167. Neely III, R. R., Marsh, D. R., Smith, K. L., Davis, S. M. & Polvani, L. M. Biases in southern hemisphere climate trends induced by coarsely specifying the temporal resolution of stratospheric ozone. *Geophysical Research Letters* **41**, 8602–8610 (2014).

168. Eyring, V. *et al.* Overview of the Coupled Model Intercomparison Project Phase 6 (CMIP6) experimental design and organization. *Geoscientific Model Development* **9**, 1937–1958 (2016).

169. Young, P. J., Davis, S. M., Hassler, B., Solomon, S. & Rosenlof, K. H. Modeling the climate impact of Southern Hemisphere ozone depletion: The importance of the ozone data set. *Geophysical Research Letters* **41**, 9033–9039 (2014).

170. Ahn, M.-S. *et al.* MJO Propagation Across the Maritime Continent: Are CMIP6 Models Better Than CMIP5 Models? *Geophysical Research Letters* **47**, e2020GL087250 (2020).

171. Chen, G., Ling, J., Zhang, R., Xiao, Z. & Li, C. The MJO From CMIP5 to CMIP6: Perspectives From Tracking MJO Precipitation. *Geophysical Research Letters* **49**, e2021GL095241 (2022).

172. Le, P. V. V., Guilloteau, C., Mamalakis, A. & Foufoula-Georgiou, E. Underestimated MJO Variability in CMIP6 Models. *Geophys Res Lett* **48**, e2020GL092244 (2021).

173. Li, Y., Wu, J., Luo, J.-J. & Yang, Y. M. Evaluating the Eastward Propagation of the MJO in CMIP5 and CMIP6 Models Based on a Variety of Diagnostics. *Journal of Climate* **35**, 1719–1743 (2022).

174. Wang, J., DeFlorio, M. J., Kim, H., Guirguis, K. & Gershunov, A. CMIP6 projections of future MJO changes under steepened moisture gradient conditions over the Indo-Pacific warm pool. (2023) doi:10.22541/essoar.167979652.29199706/v1.

175. Cavicchia, L. *et al.* Future Changes in the Occurrence of Hybrid Cyclones: The Added Value of Cyclone Classification for the East Australian Low-Pressure Systems. *Geophysical Research Letters* **47**, e2019GL085751 (2020).

176. Luca, A. D., Evans, J. P., Pepler, A. S., Alexander, L. V. & Argüeso, D. Evaluating the representation of Australian East Coast Lows in a regional climate model ensemble. *JSHESS* **66**, 108–124 (2016).

177. Pepler, A. & Dowdy, A. Fewer deep cyclones projected for the midlatitudes in a warming climate, but with more intense rainfall. *Environ. Res. Lett.* **16**, 054044 (2021).

178. Pepler, A. S. & Dowdy, A. J. Australia's Future Extratropical Cyclones. *Journal of Climate* **35**, 7795–7810 (2022).

179. Pepler, A. S. *et al.* Projected changes in east Australian midlatitude cyclones during the 21st century. *Geophysical Research Letters* **43**, 334–340 (2016).

180. Priestley, M. D. K. *et al.* An Overview of the Extratropical Storm Tracks in CMIP6 Historical Simulations. *Journal of Climate* **33**, 6315–6343 (2020).

181. Priestley, M. D. K. & Catto, J. L. Future changes in the extratropical storm tracks and cyclone intensity, wind speed, and structure. *Weather and Climate Dynamics* **3**, 337–360 (2022).

182. Grose, M. R., Fox-Hughes, P., Harris, R. M. B. & Bindoff, N. L. Changes to the drivers of fire weather with a warming climate – a case study of southeast Tasmania. *Climatic Change* **124**, 255–269 (2014).

183. Hasson, A. E. A., Mills, G. A., Timbal, B. & Walsh, K. Assessing the impact of climate change on extreme fire weather events over southeastern Australia. *Climate Research* **39**, 159–172 (2009).

184. Di Virgilio, G. *et al.* Realised added value in dynamical downscaling of Australian climate change. *Clim Dyn* **54**, 4675–4692 (2020).

185. Evans, J. P. *et al.* Design of a regional climate modelling projection ensemble experiment – NARCliM. *Geoscientific Model Development* **7**, 621–629 (2014).

186. Evans, J. P. *et al.* The CORDEX-Australasia ensemble: evaluation and future projections. *Clim Dyn* **57**, 1385–1401 (2021).

187. Espinoza, V., Waliser, D. E., Guan, B., Lavers, D. A. & Ralph, F. M. Global Analysis of Climate Change Projection Effects on Atmospheric Rivers. *Geophysical Research Letters* **45**, 4299–4308 (2018).

188. Ma, W., Chen, G. & Guan, B. Poleward Shift of Atmospheric Rivers in the Southern Hemisphere in Recent Decades. *Geophysical Research Letters* **47**, e2020GL089934 (2020).

189. Pepler, A. Projections of synoptic anticyclones for the twenty-first century. *Clim Dyn* (2023) doi:10.1007/s00382-023-06728-4.